Marise Westbroek

Ion Distributions near an Oil-Water Interface

surface tension, antagonistic salt, and external voltages

Bachelor Thesis

Supervised by Prof. dr. René van Roij

June 2013

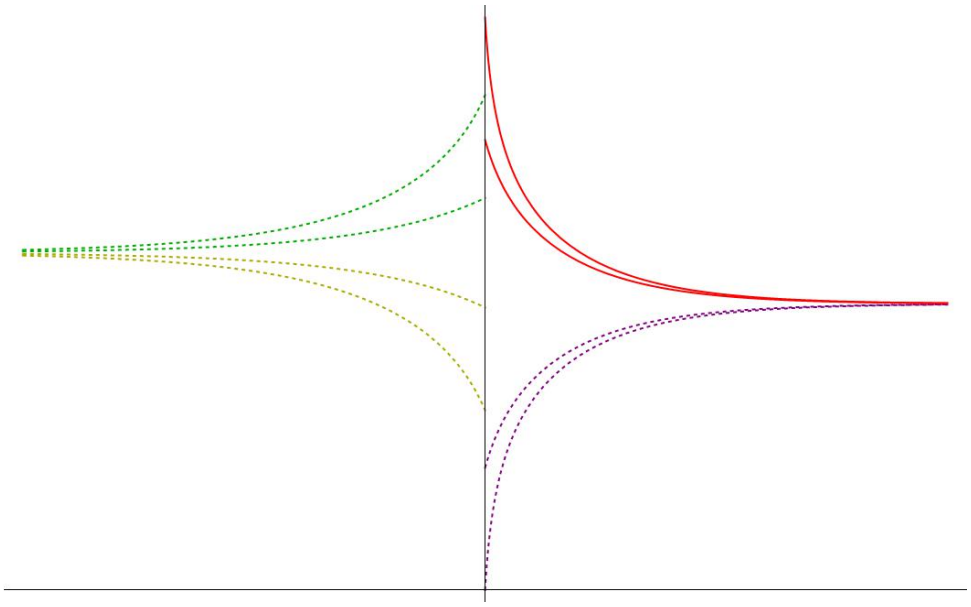

Institute for Theoretical Physics

Utrecht University

Contents

1 Introduction

The arrangement of ions at the charged interface of two immiscible liquids is crucial to many nanometer scale assembly processes in electrochemistry and biology, such as electron and ion transfer across charged biomembranes. The specific distribution of ions is also exploited in energy storage devices, where it influences the charging properties of supercapacitors.

In this thesis ion distributions are predicted by means of Poisson-Boltzmann theory. In its simplest form the Poisson-Boltzmann equation, which strongly builds upon Gouy-Chapman's treatment of a single planar charged surface in contact with a half space of electrolyte, describes the interaction of point-like ions in a structureless continuum solvent via their self-consistent mean field.

A recent experimental study of ion concentrations near an electrified oil-water interface provided the inspiration for an extension of this classical analysis. The ionic self-energy differences in oil and water, as well as the presence of two planar walls (rather than one) are incorporated to describe the ion distributions near an oil-water interface within an electrolytic cell. A schematic representation of such a cell is given below.

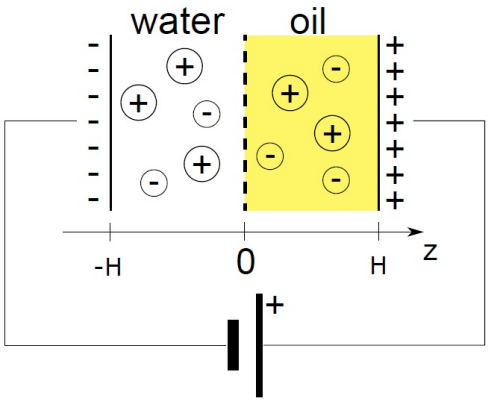

Figure 1.1: Schematic depiction of an electrolytic cell [4]

2 Electrostatic Forces

Salts easily dissociate into monovalent ions in solvents where the Coulombic attractions are weak, i.e. solvents with a high dielectric constant ϵ. Dissociation is caused by the entropy gain involved.

2.1 The Bjerrum and Debye lengths

When two monovalent ions are a distance λ_B apart their Coulombic interaction is exactly kT, where k is the Boltzmann constant and T the absolute temperature. The Bjerrum length λ_B is a property of the solvent. In Gaussian units it is given by

$$\lambda_B = \frac{e^2}{\epsilon kT}. \tag{2.1}$$

The Bjerrum length in water is 0.72 nm at room temperature.

A unit charge e in ionic solution in equilibrium is surrounded by a cloud of net negative charge, which reduces its electric field. This effect is known as Debye shielding and takes place on a typical length scale called the Debye length

$$\kappa^{-1} = \sqrt{\frac{\varepsilon kT}{8\pi e^2 \rho_s}}. \tag{2.2}$$

At fixed temperature κ^{-1} is a function of the solvent and the bulk ion concentration ρ_s. For a solution of monovalent ions in water at room temperature we have $10^{-7} < \rho_s(M) < 10$. The corresponding Debye lengths, which are given in table 2.1, range from 0.096 to 960 nm [12].

ρ_s[M]	κ^{-1}[nm]
10^{-7}	960
10^{-5}	96
10^{-3}	9.6
10^{-1}	0.96
10^{+1}	0.096

3 Poisson-Boltzmann Theory

Summary

We consider a system of monovalent ions in a dielectric continuum of dielectric constant ϵ at temperature T. The cations and anions interact with each other according to a Coulombic pair potential. In this section we present a result known as the Poisson-Boltzmann equation, which involves a nonlinear differential equation for the electrostatic potential. For the purpose of this thesis we restrict our attention to PB theory near a planar electrode. An analytic solution to the Poisson-Boltzmann equation for this planar geometry is known and will be generalized to predict ion distributions in a cell bounded by two planar electrodes in later chapters. The adsorption of ions on the electrode and the interfacial tension will be discussed briefly.

3.1 General grand potential functional

We describe a system of monovalent ions with densities $\rho_\pm(\mathbf{r})$, bulk density ρ_s and an external fixed charge density $q(\mathbf{r})$. Note that all densities are number densities, hence $\rho_+(\mathbf{r})$ provides a charge density $e\rho_+(\mathbf{r})$.

Assuming that long range pair interactions obey the Coulomb law we have the general grand potential functional [12]

$$\begin{aligned}\beta\Omega[\{\rho_\alpha\}] &= \int_V \mathrm{d}\mathbf{r}\rho_+(\mathbf{r})\left[\log\left(\rho_+(\mathbf{r})\Lambda_+^3\right)-1\right]+\int_V \mathrm{d}\mathbf{r}\rho_-(\mathbf{r})\left[\log\left(\rho_-(\mathbf{r})\Lambda_-^3\right)-1\right]\\ &+ \frac{\lambda_B}{2}\int_V \mathrm{d}\mathbf{r}\mathrm{d}\mathbf{r'}\frac{Q_+(\mathbf{r})Q_+(\mathbf{r'})}{|\mathbf{r}-\mathbf{r'}|}+\beta\int_V \mathrm{d}\mathbf{r}[\rho_+(\mathbf{r})(V_+(\mathbf{r})-\mu_+)+\rho_-(\mathbf{r})(V_-(\mathbf{r})-\mu_-)],\end{aligned} \tag{3.1}$$

where $Q(\mathbf{r})=\rho_+(\mathbf{r})-\rho_-(\mathbf{r})+q(\mathbf{r})$ is the total charge density and $V_\pm(\mathbf{r})$ is a non-electrostatic external potential.

The dimensionless electrostatic potential ϕ is given by $\beta e\psi$, with ψ the potential in volts.

$$\phi(\mathbf{r})=\lambda_B\int_V \mathrm{d}\mathbf{r'}\frac{Q(\mathbf{r'})}{|\mathbf{r}-\mathbf{r'}|}. \tag{3.2}$$

This dimensionless potential expresses an energy in terms of kT and is easily converted into ψ by the relation $\phi=1\Leftrightarrow\psi=25$ mV. Eq. (3.2) can be rewritten in differential form,

$$\nabla^2\phi(\mathbf{r})=-4\pi\lambda_B Q(\mathbf{r}),$$

where we have used that $\nabla\frac{1}{|\mathbf{r}|}=-4\pi\delta(\mathbf{r})$. This relation is known as the Poisson equation.

Combining Eq. (3.2) with the the chemical potentials $\mu_\pm$ of an ideal gas,

$$\beta\mu_\pm=\log(\rho_s\Lambda_\pm^3), \tag{3.3}$$

Eq. (3.1) can be rewritten as

$$\begin{aligned}\beta\Omega[\{\rho_\alpha\}] &= \int_V \mathrm{d}\mathbf{r}\rho_+(\mathbf{r})\left(\frac{\rho_+(\mathbf{r})}{\rho_s}-1\right)+\int_V \mathrm{d}\mathbf{r}\rho_-(\mathbf{r})\left(\frac{\rho_-(\mathbf{r})}{\rho_s}-1\right)\\ &+ \frac{1}{2}\int_V \mathrm{d}\mathbf{r}Q(\mathbf{r})\phi(\mathbf{r})+\beta\int_V \mathrm{d}\mathbf{r}[\rho_+(\mathbf{r})V_+(\mathbf{r})+\rho_-(\mathbf{r})V_-(\mathbf{r})].\end{aligned} \tag{3.4}$$

The first two terms of Eq. (3.4) add to the entropy of an ideal gas, while the second term gives the electrostatic energy of the system. The external potentials $V_\pm(\mathbf{r})$ can be added to account for specific properties of the system. This potential will be used extensively in section 4.

3.2 The Poisson-Boltzmann equation

The equilibrium condition $\frac{\delta\Omega[\{\rho_\alpha\}]}{\delta\rho_\alpha} = 0$ yields the equilibrium distributions, known as the Boltzmann distributions

$$\rho_\pm(\mathbf{r}) = \rho_s \exp[\mp\phi(\mathbf{r}) - \beta V_\pm(\mathbf{r})]. \tag{3.5}$$

See appendix (A.1) for a derivation of these equations. Relations (3.2) and (3.5) amount to

$$\nabla^2\phi(\mathbf{r}) = 4\pi\lambda_B\left[-\rho_s\exp(\phi(\mathbf{r}) - \beta V_+(\mathbf{r})) + \rho_s\exp(\phi(\mathbf{r}) - \beta V_-(\mathbf{r}))\right] - 4\pi\lambda_B q(\mathbf{r}).$$

Setting $V_\pm(\mathbf{r}) = 0$ and requiring that ϕ goes to zero at infinity we obtain the well-known Poisson-Boltzmann equation

$$\begin{aligned} \nabla^2\phi(\mathbf{r}) &= \kappa^2\sinh\phi(\mathbf{r}) - 4\pi\lambda_B q(\mathbf{r}) \\ \lim_{\mathbf{r}\to\infty}\phi(\mathbf{r}) &= 0. \end{aligned} \tag{3.6}$$

Depending on the form of $q(\mathbf{r})$ and the geometry of the system an additional boundary condition should be added.

For future reference we calculate the equilibrium grand potential of the system by inserting the equilibrium distribution (3.5) into the functional (3.4),

$$\begin{aligned} \beta\Omega_{eq} &= \int_V \mathrm{d}\mathbf{r}\frac{\rho_s}{2}\phi(\mathbf{r})\left[\exp(\phi(\mathbf{r}) - \beta V_-(\mathbf{r})) - \exp(-\phi(\mathbf{r}) - \beta V_+(\mathbf{r}))\right] \\ &- \int_V \mathrm{d}\mathbf{r}\rho_s\left\{\left[\exp(\phi(\mathbf{r}) - \beta V_-(\mathbf{r})) + \exp(\phi(\mathbf{r}) - \beta V_+(\mathbf{r}))\right] - 2\right\} \\ &+ 2\rho_s V + \frac{1}{2}\int_V \mathrm{d}\mathbf{r}\phi(\mathbf{r})q(\mathbf{r}). \end{aligned} \tag{3.7}$$

3.3 The planar geometry

It is quite exceptional that the nonlinear PB equation can be solved analytically in the geometry of a single wall in the plane $z = 0$ in contact with an electrolyte in the half space $0 < z < \infty$. Translational symmetry in the xy plane is assumed; the electrode's presence is indicated by a fixed charge density $q(\mathbf{r}) = \sigma\delta(z)$ and by the external potential

$$\beta V_\pm(z) = \begin{cases} \infty & \text{if } z < 0 \\ 0 & \text{if } z > 0. \end{cases} \tag{3.8}$$

Combining the Boltzmann distributions as obtained from Eq. (3.5)

$$\rho_\pm(z) = \rho_s\exp(\mp\phi(z) - \beta V_\pm(z)) \tag{3.9}$$

with the Poisson equation

$$\phi''(z) = -4\pi\lambda_B Q(z), \tag{3.10}$$

which follows from Eq. (3.2), we obtain a nonlinear differential equation for $\phi(z)$, known as the Poisson-Boltzmann equation:

$$\frac{d^2}{dz^2}\phi(z) = \kappa^2\sinh\phi(z) - 4\pi\lambda_B\sigma\delta(z). \tag{3.11}$$

For $z > 0$ an analytic solution to the Poisson-Boltzmann equation can be found for the planar geometry of present interest,

$$\begin{cases} \phi''(z) = \kappa^2\sinh\phi(z) \\ \lim_{z\to\infty}\phi'(z) = 0 \\ \lim\limits_{z\downarrow 0}\phi'(z) = -4\pi\lambda_B\sigma, \end{cases} \tag{3.12}$$

where σ is the dimensionless charge density. We now derive the general solution to Eq. (3.12) [12].

We introduce the dimensionless spatial coordinate $s = \kappa z$, such that

$$\frac{d^2\phi(s)}{ds^2} = \sinh\phi(s).$$

The first boundary condition is straightforward, $\lim_{s\to\infty}\phi(s) = 0$, and given that $\frac{d\phi}{ds} = \beta e\frac{d\psi}{dz}\frac{dz}{ds} = \beta e\psi'(z)$ the second condition takes the form

$$\lim_{s\downarrow 0}\phi'(s) = \lim_{z\downarrow 0}\beta e\psi'(z)\kappa = \beta e\kappa\frac{-4\pi\sigma}{\epsilon} = \frac{-4\pi\kappa\sigma\lambda_B}{e},$$

where a prime denotes a total derivative. Multiplying both sides of the differential equation by $\frac{d\phi}{ds}$ we find

$$\begin{aligned}\frac{d\phi}{ds}\frac{d^2\phi}{ds^2} &= \frac{d\phi}{ds}\sinh\phi(s)\\ \frac{d}{ds}\left[\frac{1}{2}\left(\frac{d\phi}{ds}\right)^2 - \cosh\phi(s)\right] &= 0\\ \frac{1}{2}\left(\frac{d\phi}{ds}\right)^2 - \cosh\phi(s) &= const.\end{aligned}$$

In particular we may fix the integration constant by considering the limit $s\to\infty$,

$$\begin{aligned}\lim_{s\to\infty}\left[\frac{1}{2}\left(\frac{d\phi}{ds}\right)^2 - \cosh\phi(s)\right] &= -1\\ \left(\frac{d\phi}{ds}\right)^2 &= 2[\cosh\phi(s) - 1]\\ \frac{d\phi}{ds} &= \sqrt{4\left[\frac{1}{2}(\cosh\phi(s) - 1)\right]}\\ \frac{d\phi}{ds} &= \pm 2\sinh\left(\frac{\phi(s)}{2}\right),\end{aligned}$$

where the last step follows from the identity $\sinh(\frac{x}{2}) = \sqrt{\frac{1}{2}\left[\cosh(x) - 1\right]}$. Note that only the minus sign of $\pm$ is compatible with the boundary condition. Now observe

$$\begin{aligned}\frac{d}{ds}\log\left[\tanh\left(\frac{\phi(s)}{4}\right)\right] &= \frac{1}{\tanh\left(\frac{\phi(s)}{4}\right)}\frac{1}{\cosh^2\left(\frac{\phi(s)}{4}\right)}\frac{1}{4}\frac{d\phi}{ds} =\\ \frac{1}{4}\frac{1}{\sinh\left(\frac{\phi(s)}{4}\right)\cosh\left(\frac{\phi(s)}{4}\right)}\frac{d\phi}{ds} &= \frac{1}{2\sinh\left(\frac{\phi(s)}{2}\right)}\frac{d\phi}{ds}\end{aligned}$$

,

so that upon using $\frac{d\phi}{ds} = 2\sinh\left(\frac{\phi(s)}{2}\right)$ we find

$$\frac{d}{ds}\log\left[\tanh\left(\frac{\phi(s)}{4}\right)\right] = -1.$$

This equation is satisfied if we choose

$$\tanh\left(\frac{\phi(s)}{4}\right) = \gamma_w\exp(-s) \tag{3.13}$$

where γ_w is an integration constant. From Eq. (3.13) we have, substituting $s = \kappa z$,

$$\phi(z) = 4\,\mathrm{arctanh}[\gamma_w \exp(-\kappa z)],$$

or equivalently

$$\phi(z) = 2\log\left[\frac{1+\gamma_w\exp(-\kappa z)}{1-\gamma_w\exp(-\kappa z)}\right], \tag{3.14}$$

and

$$\phi'(z) = \frac{-4\kappa\gamma_w}{\exp(\kappa z) - \gamma_w^2\exp(-\kappa z)},$$

where a prime denotes a derivative with respect to z. Finally, from

$$\lim_{z\downarrow 0}\phi'(z) = \frac{-4\kappa\gamma_w}{1-\gamma_w^2} = -4\pi\lambda_B\sigma$$

we obtain

$$\gamma_w(\sigma) = \frac{\sqrt{(2\pi\lambda_B\kappa^{-1}\sigma)^2+1}-1}{2\pi\lambda_B\kappa^{-1}\sigma}. \tag{3.15}$$

Eq. (3.15) is equivalent to

$$\sigma = \frac{8\rho_s}{\kappa}\frac{\gamma_w}{1-\gamma_w^2}. \tag{3.16}$$

Combination of relation (3.9) and solution (3.14) yields the equilibrium density profiles

$$\rho_\pm(z) = \rho_w\left[\frac{1\mp\gamma_w\exp(-\kappa z)}{1\pm\gamma_w\exp(-\kappa z)}\right]^2. \tag{3.17}$$

The grand potential can be determined from Eq. (3.7)

$$\frac{\beta\Omega(T,V,\rho_s)}{A} = 2\rho_s\int_0^\infty \mathrm{dz}\left[\frac{1}{2}\phi(z)\sinh(z) - \cosh\phi(z) - 1\right] + \frac{1}{2}\int_0^\infty \mathrm{dz}\delta(z)\sigma\phi(z) + 2\frac{\rho_s V}{A}. \tag{3.18}$$

3.4 Interfacial tension electrode-water

It is straightforward to simplify the equilibrium potential (3.7) for the planar geometry under consideration

$$\beta\Omega_{eq} = A\rho_s\int_0^\infty \mathrm{dz}\,\{\phi(z)\sinh(\phi(z)) - 2[\cosh(\phi(z))-1]\} - 2\rho_s V + \frac{A}{2}\sigma\phi(0).$$

This potential can be written as $\beta\Omega_{eq} = -pV\beta + \beta\gamma A$ with $p = 2\rho_s kT$ the bulk osmotic pressure of the electrolyte and $V = A\int_o^\infty \mathrm{dz}$ its volume, and γ the surface tension given by

$$\beta\gamma = \rho_s\int_0^\infty \mathrm{dz}\{\phi(z)\sinh(\phi(z)) - 2[\cosh(\phi(z))-1]\} + \frac{1}{2}\sigma\phi(0).$$

Substituting $s = \kappa z$ and using the relation [12]

$$\int \mathrm{ds}\left[(\Xi(s)^2 - \Xi(s)^{-2})\log\Xi(s) - \Xi(s)^2 - \Xi(s)^{-2} + 2\right] = \frac{8\gamma_w(2\gamma_w - \exp(s)\log\Xi(s))}{\exp(2s)-\gamma_w^2} + const.$$

where we have substituted $\Xi(s) = \frac{1+\gamma_w\exp(-s)}{1-\gamma\exp(-s)}$, or equivalently $\phi(s) = 2\log\Xi(s)$. Inserting the solution to the nonlinear PB equation 3.14 yields

$$\beta\gamma = \frac{\rho_s}{\kappa}\int \mathrm{ds}\left[(\Xi(s)^2 - \Xi(s)^{-2})\log\Xi(s) - \Xi(s)^2 - \Xi(s)^{-2} + 2\right]$$

$$= \frac{\rho_s}{\kappa}\frac{8\gamma_w(2\gamma_w - \exp(\kappa z)\frac{\phi(z)}{2})}{\exp(2\kappa z - \gamma_w^2)}\Big|_0^\infty = \frac{\rho_s}{\kappa}8\gamma_w\left[\frac{\log\left(\frac{1+\gamma_w}{1-\gamma_w}\right) - 2\gamma_w}{1-\gamma_w^2}\right].$$

This is an explicit expression for the surface tension γ as a function of ρ_s, λ_B and σ, since the integration constant γ_w depends on these quantities through Eq. (3.15). Fig. 3.1 shows $\gamma(\sigma)$ for $\lambda_B = 0.72$ nm (water), for $\rho_s = 1$ M, $\rho_s = 100$ mM and $\rho_s = 10$ mM. The interfacial tension is, like the electrostatic potential, defined up to a constant. The presence of salt impedes the increase of the surface tension with the charge density σ.

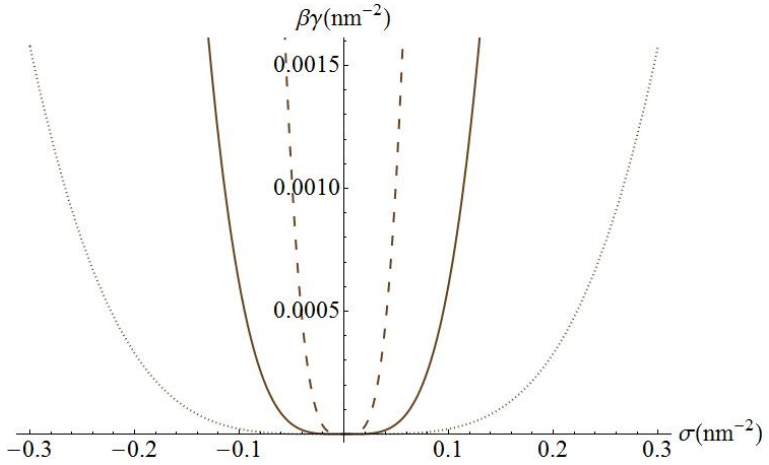

Figure 3.1: Interfacial tension electrode-water $\beta\gamma$ as a function of the charge density σ, for $\rho_s = 1$ M (dotted line), $\rho_s = 100$ mM (thick line) and $\rho_s = 10$ mM (dashed line). The interfacial tension grows faster with σ for lower salt concentrations.

3.5 Adsorptions $\Gamma_\pm$

To describe the excess number of ions near the electrode we introduce the adsorptions

$$\Gamma_\pm = \int_0^\infty \mathrm{dz}(\rho_\pm(z) - \rho_s). \tag{3.19}$$

Using the expressions for the equilibrium densities (3.17) we find

$$\Gamma_\pm = \int_0^\infty \mathrm{dz}\rho_s \left\{ \left[\frac{1 \mp \gamma_w \exp(-\kappa z)}{1 \pm \gamma_w \exp(-\kappa z)} \right]^2 - 1 \right\} = \frac{\mp\rho_s}{\kappa} \frac{4\gamma_w}{1 \pm \gamma_w}.$$

One checks that the electrode is electrically neutral:

$$\Gamma_+ - \Gamma_- = \frac{-4\gamma_w}{1-\gamma_w^2} \frac{2\rho_s}{\kappa} = \frac{-4\pi\lambda_B\sigma}{\kappa} \frac{2\rho_s}{\kappa} = -\sigma. \tag{3.20}$$

4 Salts near Dielectric Interfaces

Summary

This chapter will focus on the equilibrium distributions of ions near an oil-water interface. Solvation energies are illustrated by the Born energy and are defined as step functions with a discontinuity at the interface. As a consequence of these self-energy differences the ions will partition unequally between water and oil. A modified Poisson-Boltzmann theory is introduced for the dielectric interface. Special attention is paid to the interfacial tension.

4.1 Born energy

An ion in a medium has an electrostatic free energy associated with it, even when not interacting with other ions - the so-called self-energy. This energy is equal to the electrostatic work done in forming the ion. For spherical particles in a medium it is commonly referred to as the Born energy. This quantity determines the extent to which ions will dissolve and partition in different solvents. It will play an important role in the rest of this thesis.

Consider the process of charging a spherical ion of radius a, located at the origin, by gradually increasing its charge from 0 to its full charge e. If the charge at any time t is given by $q(t)$ and is increased by dq the work done in bringing this additional charge from infinity to $r = a$ is given by Coulomb's law [5]

$$dw = \frac{qdq}{4\pi\epsilon_0\epsilon a} \tag{4.1}$$

and hence the Born energy is given by

$$\int \mathrm{dw} = \int_0^e \mathrm{dq} \frac{q}{4\pi\epsilon_0\epsilon a} = \frac{e^2}{8\pi\epsilon_0\epsilon a}. \tag{4.2}$$

The specific form of the Born energy will not be assumed the rest of this thesis. Rather, an ion's generic self-energy will be described as a step function across the interface between oil and water, gauged at zero in water and taking a constant value $f_\pm$ in oil, where the index $\pm$ refers to the particle's charge. If the self-energies of cat- and anions have opposite signs the salt is called antagonistic. We will deal with this type of salt extensively in section (5).

4.2 Poisson-Boltzmann theory near the interface

We consider a planar geometry with half spaces $z < 0$ and $z > 0$ filled with water and oil, respectively. The liquids are assumed to be homogeneous, structureless dielectric media with respective dielectric constants ϵ_w and ϵ_o. They form a flat interface at $z = 0$. From the generic grand potential functional [2],

$$\beta\Omega[\{\rho_\alpha\}] = \sum_{\alpha=\pm} \int \mathrm{d}\mathbf{r}\rho_\pm(\mathbf{r}) \left[\log\left(\frac{\rho_\pm(\mathbf{r})}{\rho_s}\right) - 1\right] + \frac{1}{2}\int \mathrm{d}\mathbf{r}Q(\mathbf{r})\phi(\mathbf{r}) + \sum_{\alpha=\pm}\int \mathrm{d}\mathbf{r}\rho_\alpha(\mathbf{r})\beta V_\alpha(\mathbf{r}), \tag{4.3}$$

where $Q(\mathbf{r}) = \rho_+(\mathbf{r}) - \rho_-(\mathbf{r}) + q(\mathbf{r})$ is the total charge density, $\phi(\mathbf{r})$ is the dimensionless electrostatic potential and ρ_s denotes the bulk concentration at $\lim_{z\to\infty}$ in water. Eq. (4.3) can be rewritten for the planar geometry of present interest as

$$\beta\Omega[\{\rho_\alpha\}] = \sum_{\alpha=\pm} A\int_{-\infty}^{\infty} \mathrm{dz}\rho_\alpha(z) \left[\log\left(\frac{\rho_\alpha(z)}{\rho_s}\right) - 1 + \beta V_\alpha(z) + \frac{\alpha}{2}\phi(z,[\{\rho_\alpha\}])\right], \tag{4.4}$$

in terms of the dimensionless electrostatic potential $\phi(z,[\{\rho_\alpha\}])$ and the external potential

$$V_\pm(z) = \begin{cases} 0 & \text{if } z < 0 \\ f_\pm & \text{if } z > 0. \end{cases} \tag{4.5}$$

The self-energies f_+ of cations (charge e) and f_- of anions (charge $-e$) have been gauged to zero in water. The equilibrium conditions can be found by minimizing the functional (4.4), which gives

$$\rho_\pm(z) = \rho_w \exp(-\beta V_\pm(z) \mp \phi(z)). \tag{4.6}$$

These account for the Poisson-Boltzmann equations in terms of the Debye lengths $\kappa_{w,o}$ in water and oil,

$$\phi''(z) = \begin{cases} \kappa_w^2 \sinh(\phi(z)) & \text{if } z < 0 \\ \kappa_o^2 \sinh(\phi(z) - \phi_D) & \text{if } z > 0, \end{cases} \tag{4.7}$$

where the Donnan potential ϕ_D is given by $\phi_D = \frac{1}{2}(f_- - f_+)$. The corresponding boundary conditions read

$$\begin{aligned} \lim_{z\uparrow 0} \phi(z) &= \lim_{z\downarrow 0} \phi(z) \\ \lim_{z\uparrow 0} \epsilon_w \phi'(z) &= \lim_{z\downarrow 0} \epsilon_o \phi'(z) \\ \lim_{z\to-\infty} \phi'(z) &= \lim_{z\to\infty} \phi'(z) = 0. \end{aligned} \tag{4.8}$$

In the set (4.7) the Donnan potential ϕ_D appears in the argument of the sinh. This potential is determined as follows. In the limits $\lim_{z\to-\infty}$ and $\lim_{z\to\infty}$ we require $\rho_+ = \rho_-$ by neutrality of bulk fluids.Denoting

the potentials in these limits by

- $\lim_{z\to-\infty} \phi(z) \equiv \phi_W$
- $\lim_{z\to\infty} \phi(z) \equiv \phi_D$

we find that in water $\exp(-\phi_W) = \exp(\phi_W)$, which implies $\phi_W = 0$. In oil we have $\exp(-f_+ - \phi_D) = \exp(-f_- + \phi_D)$, hence

$$\phi_D = \frac{1}{2}(f_- - f_+). \tag{4.9}$$

The general solution to Eq. (4.7) with the boundary conditions of Eq. (4.8) is given by

$$\phi(z) = \begin{cases} 2\log\left[\dfrac{1 + C_w \exp(\kappa_w z)}{1 - C_w \exp(\kappa_w z)}\right] & \text{if } z < 0 \\ 2\log\left[\dfrac{1 + C_o \exp(-\kappa_o z)}{1 - C_o \exp(-\kappa_o z)}\right] + \phi_D & \text{if } z > 0. \end{cases} \tag{4.10}$$

The integration constants C_w en C_o follow from the boundary conditions at $z = 0$ as

$$C_w = \frac{\kappa_o + \exp(\phi_D)\kappa_o + 2\exp(\frac{\phi_D}{2})\kappa_w \frac{\epsilon_w}{\epsilon_o} - 2\sqrt{\exp(\phi_D)(\kappa_o^2 + \kappa_w^2(\frac{\epsilon_w}{\epsilon_o})^2 + 2\kappa_o\kappa_w \frac{\epsilon_w}{\epsilon_o}\cosh(\frac{\phi_D}{2})}}{\kappa_o(\exp(\phi_D) - 1)} \tag{4.11}$$

$$C_o = -\frac{\kappa_w \frac{\epsilon_w}{\epsilon_o} + \exp(\phi_D)\kappa_w \frac{\epsilon_w}{\epsilon_o} + 2\kappa_o \exp(\frac{\phi_D}{2}) - 2\sqrt{\exp(\phi_D)(\kappa_o^2 + \kappa_w^2(\frac{\epsilon_w}{\epsilon_o})^2 + 2\kappa_o\kappa_w \frac{\epsilon_w}{\epsilon_o}\cosh(\frac{\phi_D}{2})}}{\kappa_w(\exp(\phi_D) - 1)} \tag{4.12}$$

In oil we have that $\rho_\pm(z) = \rho_w \exp(f_\pm \mp \phi(z)$. Using Eq. (4.10) we can rewrite this as

$$\rho_\pm(z) = \rho_w \left[\frac{1 \mp C_o \exp(\kappa_o z)}{1 \pm C_o \exp(-\kappa_o z)}\right]^2 \exp(-f_\pm \mp \phi_D) \tag{4.13}$$

where

$$\rho_o = \rho_w \exp(f_\pm \mp \phi_D), \tag{4.14}$$

so that the densities in oil are given by

$$\rho_\pm(z) = \rho_o \exp[\mp(\phi(z) - \phi_D)]. \tag{4.15}$$

The equilibruim concentrations follow from Eq. (4.6)

$$\rho_{\pm}(z) = \begin{cases} \rho_w \left[\dfrac{1 \mp C_w \exp(\kappa_w z)}{1 \pm C_w \exp(\kappa_w z)}\right]^2 & \text{if } z < 0 \\ \rho_o \left[\dfrac{1 \mp C_o \exp(\kappa_o z)}{1 \pm C_o \exp(\kappa_o z)}\right]^2 & \text{if } z > 0. \end{cases} \tag{4.16}$$

Typical density profiles are shown in figure 5.2. Due to preferential partitioning a net charge is found in the water phase, in a narrow band near the interface of approximate width κ_w^{-1}. This is compensated by an opposite net charge in the oil phase in a band of width $\simeq \kappa_o^{-1}$.

The charge density σ_w that acculumuates in the water phase can be calculated from the Poisson-Boltzmann equations and their boundary conditions

$$\begin{aligned} \sigma_w &= \int_{-\infty}^{0} \mathrm{dz}(\rho_+(z) - \rho_-(z)) = -2\rho_w \int_{-\infty}^{0} \mathrm{dz}\sinh(\phi(z)) = \frac{-2\rho_w}{\kappa_w^2} \int_{-\infty}^{0} \mathrm{dz}\phi''(z) \\ &= \frac{-2\rho_w}{\kappa_w^2} \left[\phi'(z)\right]_{-\infty}^{0} = \frac{-2\rho_w}{\kappa_w^2} \lim_{z\uparrow 0} \phi'(z) = -\frac{8\rho_w}{\kappa_w} \frac{C_w}{1 - C_w^2}. \end{aligned} \tag{4.17}$$

In Fig. 4.1 the charge accumulation near the interface is shown as a function of the bulk concentration in water for self-energies $f_{\mp} = (0, 6)$ kT, $f_{\mp} = (-3, 3)$ kT, $f_{\mp} = (-6, 6)$ kT. There is more interfacial excess charge in the case of antagonistic salts, as will be discussed in section 5.

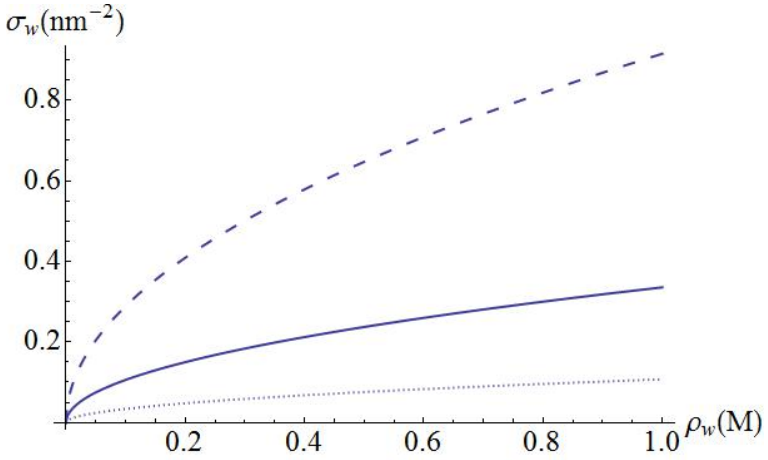

Figure 4.1: Charge accumulation σ_w at the water side of the interface as a function of the bulk concentration ρ_s in water, for self-energies $(f_-, f_+) = (0, 6)$ kT (dotted line), $(f_-, f_+) = (-3, 3)$ kT (thick line), $(f_-, f_+) = (-6, 6)$ kT (dashed line).

4.3 Interfacial tension oil-water

The electrostatic component of the interfacial tension will be denoted by γ.

We have so far considered the grand-canonical (μ, V, T) ensemble. The grand-canonical potential of a bulk system depends linearly on the volume via

$$\Omega(\mu, V, T) = -Vp(\mu, T), \tag{4.18}$$

where p is the pressure. In the particular case of the planar geometry we have $V = V_w + V_o$ and $p = p_w + p_o$, where p_w is the pressure in the half space $z < 0$. Following the ideal gas law we have $p_w = 2k_BT\rho_w$. Denoting the area of the interface by A the grand potential Ω can be split in three terms

$$\Omega(\mu, Vo, Vw, A, T) = -p_w(\mu, T)V_w - p_o(\mu, T)V_o + \gamma(\mu, T)A. \tag{4.19}$$

From this equation we see that γ can be found from

$$\beta A\gamma = \beta\Omega[\{\rho_\alpha\}]_{\rho=\rho_{eq}} - \beta\Omega[\{\rho_\alpha\}]_{\rho=\rho_{o,w}}. \tag{4.20}$$

We can now use Eq. (4.4). Noting that the electrostatic potential equals zero in bulk electrolyte,

$$\begin{aligned}\beta\gamma = &\int_{-\infty}^{0} \mathrm{d}z\rho_+(z)\left[\log\left(\frac{\rho_+(z)}{\rho_w}\right) - 1 + \frac{1}{2}\phi(z)\right] + \int_{-\infty}^{0} \rho_-(z)\left[\log\left(\frac{\rho_-(z)}{\rho_w}\right) - 1 - \frac{1}{2}\phi(z)\right] \\ &-2\int_{-\infty}^{0} \mathrm{d}z\rho_w\left[\log\left(\frac{\rho_w}{\rho_w}\right) - 1\right] \\ &+\int_{0}^{\infty} \mathrm{d}z\rho_+(z)\left[\log\left(\frac{\rho_+(z)}{\rho_o}\right) - 1 + \frac{1}{2}\phi(z)\right] + \int_{0}^{\infty} \rho_-(z)\left[\log\left(\frac{\rho_-(z)}{\rho_w}\right) - 1 - \frac{1}{2}\phi(z)\right] \\ &-2\int_{0}^{\infty} \mathrm{d}z\rho_o\left[\log\left(\frac{\rho_o}{\rho_o}\right) - 1\right]\end{aligned} \tag{4.21}$$

or equivalently

$$\begin{aligned}\beta\gamma = &- \int_{-\infty}^{0} \mathrm{d}z(\rho_{+,eq}(z) + \rho_{-,eq}(z) - 2\rho_w) - \int_{0}^{\infty} \mathrm{d}z(\rho_{+,eq}(z) + \rho_{-,eq}(z) - 2\rho_o) \\ &- \frac{1}{2}\int_{-\infty}^{0} \mathrm{d}z\phi(z)(\rho_{+,eq}(z) - \rho_{-,eq}(z)) - \frac{1}{2}\int_{0}^{\infty} \mathrm{d}z\phi(z)(\rho_{+,eq}(z) - \rho_{-,eq}(z)).\end{aligned} \tag{4.22}$$

Inserting the equilibrium density profiles (4.6) and combining these with relations (4.9) and (4.14) yields

$$\begin{aligned}\beta\gamma = &- \int_{-\infty}^{0} \mathrm{d}z\,\{2\rho_w[\cosh(\phi(z)) - 1]\} - \int_{0}^{\infty} \mathrm{d}z\,\{2\rho_o[\cosh(\phi(z) - \phi_D) - 1]\} \\ &+ \int_{-\infty}^{0} \mathrm{d}z\phi(z)\sinh(\phi(z)) + \int_{0}^{\infty} \mathrm{d}z\phi(z)\sinh(\phi(z) - \phi_D).\end{aligned} \tag{4.23}$$

The integrands are plotted in Fig. 5.4, which shows the effect of the self-energies on the surface tension. Expression (4.23) will be adapted in section 11.1, where it is used to calculate the oil-water interfacial tension within an electrolytic cell.

5 Antagonism

Summary

In this section our attention will be restricted to the oil-water interface. The grand-canonical ensemble is be used to describe the system of interest. Ionic equilibrium distributions near an oil-water interface are calculated by means of a non-linear Poisson-Boltzmann theory. Antagonistic salts, characterized by different signs of the self-energies $f_{\alpha\pm}$, are compared to non-antagonistic salts. Antagonism is found to lead to a small Debye length. Antagonistic salts are shown to make a negative contribution to the surface tension.

5.1 Potential and density profiles

5.1.1 Influence of the self-energies

The oil-water interface is located in the plane $z = 0$ and separates water ($z < 0$) and oil ($z > 0$). Both solvents will be treated as structureless media of dielectric constants ϵ_w and ϵ_o, respectively. In the grand-canonical ensemble the bulk density ρ_w far from the interface in water is fixed [11]. For $\rho_w = 100$ mM, $\epsilon_w = 78.54$, $\epsilon_o = 5.43$ and $T = 294$ K we compare the following parameter sets:

1. $f_- = 0$, $f_+ = 6$ kT ($\kappa_o^{-1} = 1.6$ nm)
2. $f_- = -3$ kT, $f_+ = 3$ kT ($\kappa_o^{-1} = 0.35$ nm).

The cations' positive self-energies in oil give rise to a net negative charge in oil in both cases. In case 1, which is non-antagonistic, the anions have no preference for either phase; in the antagonistic case the cat- and anions have opposing interests. In equilibrium a balance is reached between the system's incompatible aims at minimal electrostatic energy and maximal entropy. The latter effect is relatively weak in the antagonistic case, resulting in a thick double layer.

From Eq. (2.2) we see that the Debye length κ_w^{-1} is uniquely determined by ρ_w, T and $\epsilon_{w,o}$. For the given parameters $\kappa_w^{-1} = 3.0$ nm. From relation (4.14) we have that $\kappa_o^2 = \kappa_w^2 \frac{\epsilon_w}{\epsilon_o} \exp[-\frac{1}{2}(f_- + f_+)]$, hence the Debye length in oil κ_o^{-1} is linear in $\sqrt{\exp[\frac{1}{2}(f_- + f_+)]}$ and will be smaller in the antagonistic case 2. From Eq. (4.14) it is immediate that the bulk density in oil ρ_o scales with $\exp[-\frac{1}{2}(f_- + f_+)]$. The

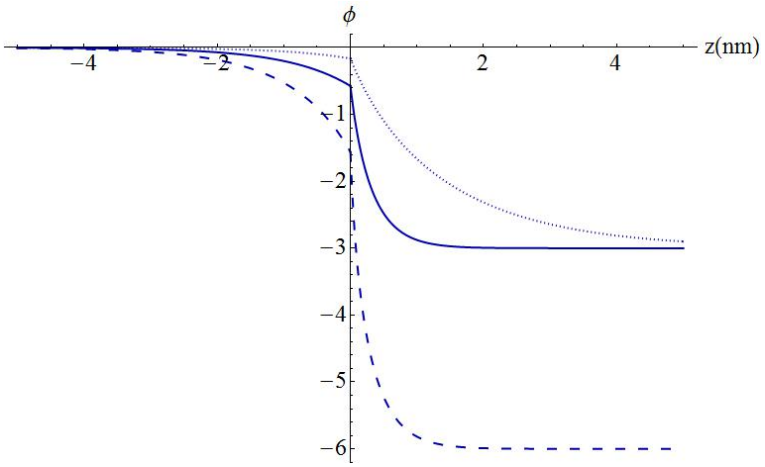

Figure 5.1: The dimensionless potential ϕ near the dielectric interface as a function of the distance z (nm), for a fixed bulk density $\rho_w = 100$ mM, dielectric constants $\epsilon_w = 78.54$, $\epsilon_o = 5.43$ and $T = 294$ K. The dotted and thick lines show a non-antagonistic salt with self-energies $(f_-, f_+) = (0, 6)$ kT and an antagonistic salt with an equal difference between f_+ and f_-, namely $(f_-, f_+) = (-3, 3)$ kT, respectively. The dashed line, which depicts the potential for self-energies $(f_-, f_+) = (-6, 6)$ kT, will be referred to in section (5.2).

density ρ_o is thus significantly higher for the antagonistic salt, as can be seen from Fig. 5.2.

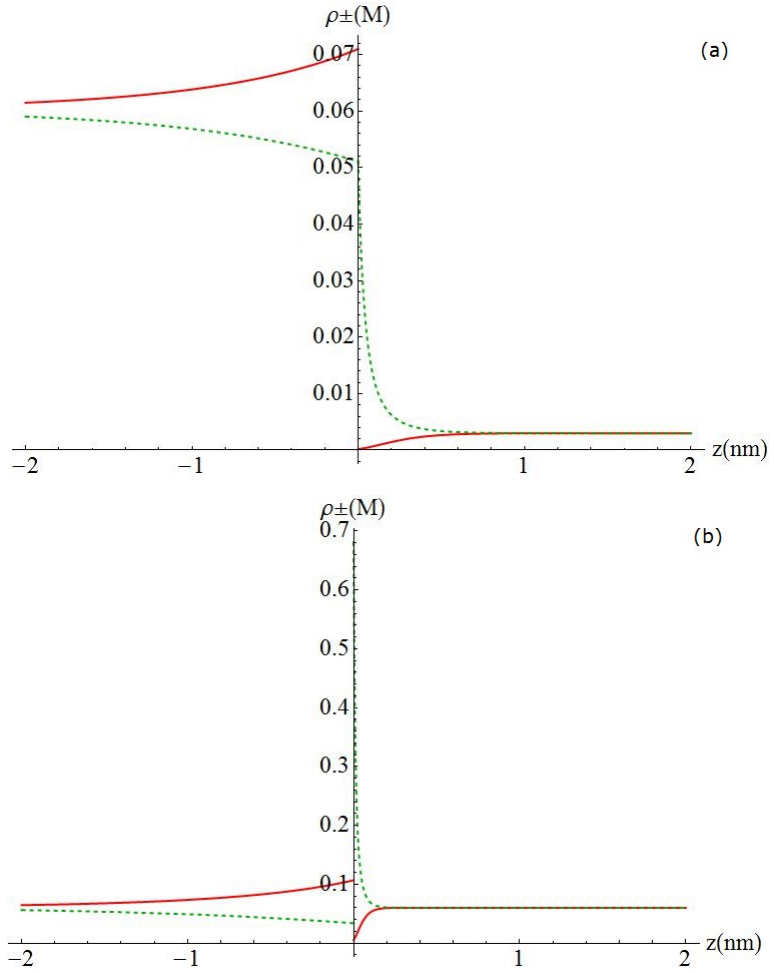

Figure 5.2: Density profiles of cations (thick lines) and anions (dashed lines) as a function of the distance z nm from the interface for self-energies $(f_-, f_+) = (0, 6)$ kT (Fig. a) and $(f_-, f_+) = (-3, 3)$ kT (Fig. b). Near the interface in water the cations have a slightly higher density than the anions, which results in a cloud of net charge with a width of less than 2 nm. The compensating charge is present in the oil.

5.1.2 Influence of the dielectric constant ϵ_o

For the antagonistic salt parameter set of section 5.1.1 we now consider the influence of the dielectric constant ϵ_o. The permittivity ϵ_o is a measure of the oil's electric susceptibility. Low values of this parameter indicate that the oil is difficult to polarize: that it only responds to the presence of an electric field to a limited extent. Since $E(z) = -\frac{d\phi}{dz}$ we gather from figure 5.3 that the electric field is positive and decreasing in the half-space $z > 0$.

Note that for $\epsilon_o = 78.54$ we have $\epsilon_w = \epsilon_o$. Since one of the boundary conditions 4.8 reads $\lim_{z\uparrow 0} \epsilon_w \phi'(z) = \lim_{z\downarrow 0} \epsilon_o \phi'(z)$ the potential ϕ is differentiable near the interface.

5.2 Effect of self-energies on interfacial tension

The ions make a net negative contribution to the interfacial tension. Antagonism enhances this effect. Antagonistic salts, which contain both hydrophilic and hydrophobic ions, resemble surfactants: they lower the surface tension, more so than their non-antagonistic counterparts. This point is illustrated by Fig. (5.1). In figure 5.4 the integrands in Eq. (4.23) are shown as a function of the distance from the interface. The antagonistic salts' small Debye lengths are compensated for by the high voltage drop across the interface. The resulting contributions to the interfacial tension $\beta\gamma$ as calculated in Eq. (4.23) are plotted as function of the salt concentration in Fig. 5.5.

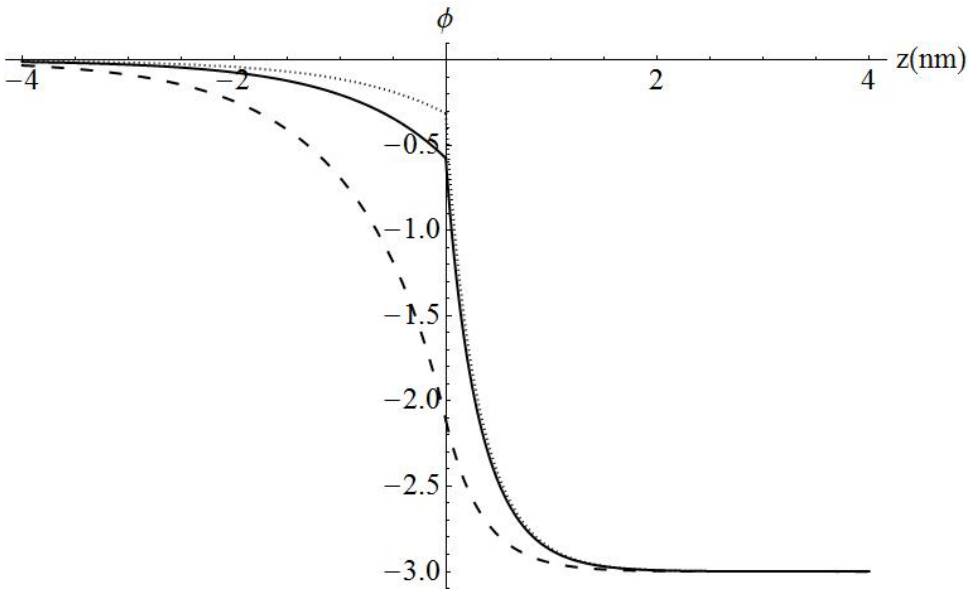

Figure 5.3: Dimensionless potential ϕ as a function of the distance z nm from the interface for bulk concentration $\rho_w = 100$ mM, self-energies $f_- = -3$ kT and $f_+ = 3$ kT and dielectric constants $\epsilon_o = 2.5$ (dashed line), $\epsilon_o = 10$ (thick line) and $\epsilon_o = 78.54$ (dotted line). For small values of ϵ_o an electric field is only present in the immediate vicinity of the interface.

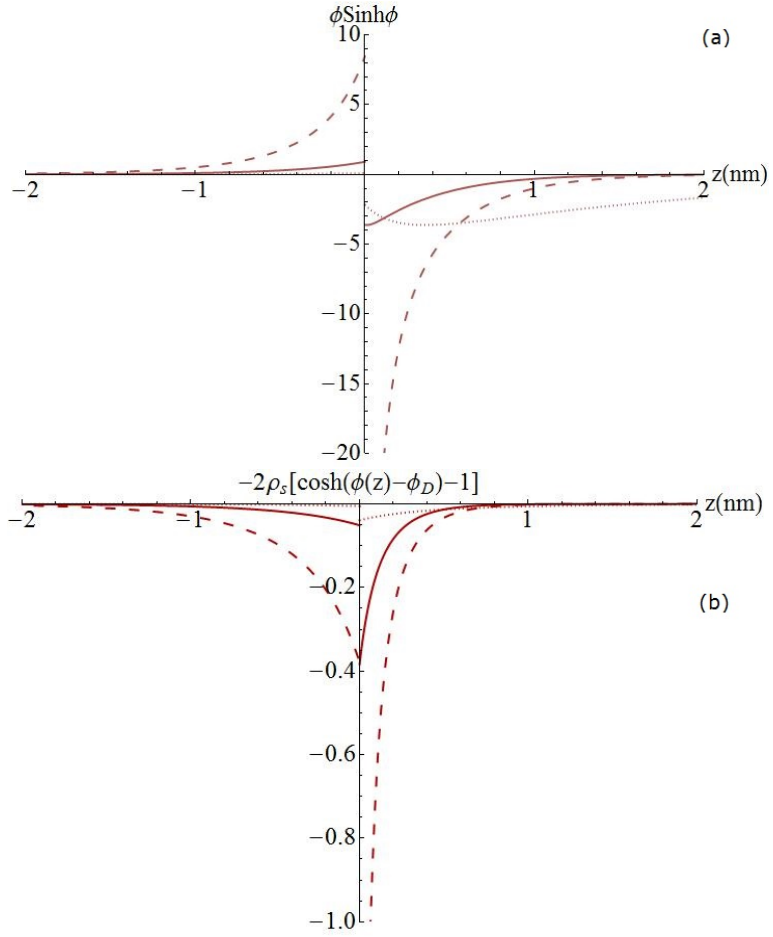

Figure 5.4: The expressions $\phi \sinh \phi$ and $-2\rho_s[\cosh(\phi - \phi_D)]$, which appear in the interfacial tension (4.23), as a function of the spatial coordinate z, for $\rho_w = 100$ mM. The dashed line corresponds to the strongly antagonistic self-energies $(f_-, f_+) = (-6, 6)$ kT and has a greater negative effect on $\beta\gamma$ than salts with self-energies $(f_-, f_+) = (-3, 3)$ kT (thick lines) or $(f_-, f_+) = (0, 6)$ kT (dotted lines).

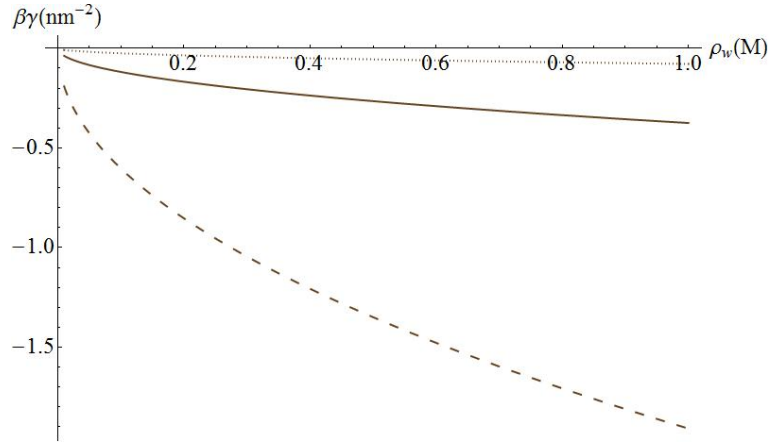

Figure 5.5: Electrostatic contribution to the interfacial tension as a function of the bulk density in water ρ_w for self-energies $(f_-, f_+) = (-6, 6)$ kT (lower dashed line), $(f_-, f_+) = (-3, 3)$ kT (thick line) and $(f_-, f_+) = (0, 6)$ kT (upper dashed line). Antagonistic salts have the greatest lowering effect on the surface tension.

6 Two planar Electrodes, two Salts

Summary

In this chapter the Poisson-Boltzmann theory developed in chapters 3 and 4 will be adapted to determine the electrostatic potential and density profiles within a finite thermodynamic system containing an oil-water interface.

6.1 System

We consider a closed system of two charged planar electrodes with area A separated by a distance H. The gap in between is filled with water ($-\frac{H}{2} < z < 0$) and oil ($0 < z < \frac{H}{2}$), with an interface located in the plane $z = 0$. We consider salt concentrations such that the Debye lengths in oil as well as in water are much smaller than $\frac{H}{2}$, such that the electric double layers of the plates and the interface are separated by a well-defined bulk electrolyte. Based on the assumption $\kappa H \gg 1$ we can apply Poisson-Boltzmann theory to ions near the electrodes and interface independently.

We use two salts and hence four types of ions. Since there is a fixed number of ions in this volume we must employ the canonical ensemble for a physically accurate description. Within this ensemble we cannot fix grand-canonical bulk densities $\rho_i^{w,o}$, where i labels the two salt species. Instead, we specify the numbers of ions $N_{i\pm} = \rho_{i\pm} AH$. The densities ρ_i will be referred to as canonical bulk densities. The resulting grand-canonical bulk densities $\rho_{i\pm}^w$ in water and $\rho_{i\pm}^o$ in oil will be such that there is charge neutrality in both phases once the system reaches equilibrium.[1] It is non-trivial to find $\rho_{i\pm}^{w,o}$ from the fixed number of ions $N_{i\pm}$, since the ions' partitioning will depend on their self-energies $f_{i\pm}$, the charge density on the left electrode σ_1, and H.

The degrees of freedom are

- Numbers of ions for both salts N_1 and N_2.
- Charge density σ_1 on the water-immersed electrode at $z = -\frac{H}{2}$, which induces an equal but opposite density on the right electrode and a density σ_2 at the water side of the interface and $-\sigma_2$ at the oil side by neutrality.
- Four self-energies $f_{i\pm}$.
- Lenght H.

6.2 Determination of the potential ϕ

Using the grand-canonical densities $\rho_{1\pm}^w$ and $\rho_{2\pm}^w$ as parameters and exploiting the PB theory discussed in sections 3.3 and 4.2 we can express the potential ϕ in terms of these unknowns. Observe that the grand-canonical bulk densities in oil depend on those in water via the corresponding self-energies and the Donnan potential. These relations, together with the requirement of charge neutrality in bulk oil, amount to five equations

$$\begin{aligned} \rho_{i\pm}^o &= \rho_{i\pm}^w \exp(-f_{i\pm} \mp \phi_D) \\ \rho_{1+}^o - \rho_{1-}^o + \rho_{2+}^o - \rho_{2-}^o &= 0. \end{aligned} \tag{6.1}$$

Solving for ϕ_D we find

$$\phi_D = \frac{1}{2}(f_{1-} + f_{2-}) \log\left[\frac{\rho_{1-}^w \exp(-f_{1+}) + \rho_{2+}^w \exp(-f_{2+})}{\rho_{1+}^w \exp(f_{2-}) + \rho_{2-}^w \exp(f_{1-})}\right]. \tag{6.2}$$

[1] This constraint is taken care of by the Donnan potential ϕ_D. Problems may arise only if all ions have a preference for a single phase because of their self-energies. We will not pursue this here.

From section 3.3 we deduce the form of the potential ϕ near either electrode

$$\phi(z) = \begin{cases} \phi^{el,w}(z) = 2\log\left\{\dfrac{1+\gamma_w \exp[-\kappa_w(z+\frac{H}{2})]}{1-\gamma_w \exp[-\kappa_w(z+\frac{H}{2})]}\right\} & \text{if } \frac{-H}{2} < z < \frac{-H}{4} \\ \phi^{o,el}(z) = 2\log\left\{\dfrac{1+\gamma_o \exp[\kappa_o(z-\frac{H}{2})]}{1-\gamma_o \exp[\kappa_o(z-\frac{H}{2})]}\right\} + \phi_D & \text{if } \frac{H}{4} < z < \frac{H}{2}. \end{cases} \tag{6.3}$$

The integration constants γ_w is fully determined by the parameters σ_1 and ρ^w_{i+}, since the boundary condition at $z = -\frac{H}{2}$ dictates that $\phi'(-\frac{H}{2}) = -4\pi\lambda_B\sigma_1$.

$$\gamma_w = \frac{\sqrt{(2\pi\lambda^w_B\kappa_w^{-1}\sigma)^2+1}-1}{2\pi\lambda^w_B\kappa_w^{-1}\sigma}. \tag{6.4}$$

Similarly, since a charge density $-\sigma_1$ accumulates at the oil-immersed electrode,

$$\gamma_o = \frac{\sqrt{(2\pi\lambda^o_B\kappa_o^{-1}(-\sigma_1))^2+1}-1}{2\pi\lambda^o_B\kappa_o^{-1}(-\sigma_1)}, \tag{6.5}$$

where $\kappa_o = \sqrt{8\pi\lambda^o_B(\rho^o_{1+}+\rho^o_{2+})}$. The integration constant γ_o is therefore also known in terms of σ_1 and the grand-canonical bulk densities in water. The Poisson-Boltzmann theory developed in section 4.2 can be applied directly. The potential near the interface is given by

$$\phi(z) = \begin{cases} \phi^{w,int}(z) = 2\log\left[\dfrac{1+C_w\exp(\kappa_w z)}{1-C_w\exp(\kappa_w z)}\right] & \text{if } \frac{-H}{4} < z < 0 \\ \phi^{int,o}(z) = 2\log\left[\dfrac{1+C_o\exp(-\kappa_o z)}{1-C_o\exp(-\kappa_o z)}\right] + \phi_D & \text{if } 0 < z < \frac{H}{4}. \end{cases} \tag{6.6}$$

Note that the potential ϕ is continuous at $z = 0$ and satisfies the boundary conditions near the interface

$$\begin{aligned} \lim_{z\uparrow 0}\phi^{w,int}(z) &= \lim_{z\downarrow 0}\phi^{int,o}(z) \\ \lim_{z\uparrow 0}\epsilon_w\phi'^{w,int}(z) &= \lim_{z\downarrow 0}\epsilon_o\phi'^{int,o}(z), \end{aligned} \tag{6.7}$$

which are met by the integration constants as given in Eq. (4.11).

6.3 Adsorptions $\Gamma^{w,o}_{i\pm}$

For the determination of the grand-canonical bulk densities in water $\rho^w_{i\pm}$ we have eight equations,

$$N_{i\pm} = \rho^w_{i\pm}\frac{AH}{2} + \rho^o_{i\pm}\frac{AH}{2} + \Gamma_{i\pm}A, \tag{6.8}$$

for $i = 1, 2, 3, 4$ and $\pm = +$ or $-$. Ions can adsorb on either electrode and on either side of the interface, so the adsorption $\Gamma_{i\pm}$ can be decomposed in the following four contributions

$$\Gamma_{i\pm} = \Gamma^{w,el}_{i\pm} + \Gamma^{w,int}_{i\pm} + \Gamma^{int,o}_{i\pm} + \Gamma^{o,el}_{i\pm},$$

yielding a total of 16 adsorption terms. By analogy with Eq. (3.19) the adsorption of type i ions on the left electrode would be given by

$$\Gamma^{w,el}_{i\pm} = \int_0^{\frac{H}{4}} \mathrm{d}z \left(\rho^w_{i\pm}\left\{\left[\frac{1\mp\gamma_w(\sigma_1)\exp(-\kappa_w z)}{1\pm\gamma_w(\sigma_1)\exp(-\kappa_w z)}\right]^2 - 1\right\}\right),$$

from which

$$\begin{aligned} \Gamma^{w,el}_{i-} &= \frac{4\gamma_w(\sigma_1)\rho^w_{i-}}{\kappa_w}\left[\frac{1}{1-\gamma_w(\sigma_1)} - \frac{1}{\exp(\frac{\kappa_w H}{4})-\gamma_w(\sigma_1)}\right] \\ \Gamma^{w,el}_{i+} &= \frac{-4\gamma_w(\sigma_1)\rho^w_{i+}}{\kappa_w}\left[\frac{1}{1+\gamma_w(\sigma_1)} - \frac{1}{\exp(\frac{\kappa_w H}{4}+\gamma_w(\sigma_1))}\right]. \end{aligned}$$

Taking the limit $\kappa H \gg 1$ we can simplify these adsorptions to

$$\begin{aligned}\Gamma_{i-}^{w,el} &= \frac{4\rho_{i-}^{w}}{\kappa_w}\frac{\gamma_w(\sigma_1)}{1-\gamma_w(\sigma_1)} \\ \Gamma_{i+}^{w,el} &= \frac{-4\rho_{i+}^{w}}{\kappa_w}\frac{\gamma_w(\sigma_1)}{1+\gamma_w(\sigma_1)}.\end{aligned}$$

The remaining twelve adsorption terms can be found by the evaluation of similar integrals,

$$\begin{aligned}\Gamma_{i\pm}^{w,int} &= \frac{\mp 4\rho_{i\pm^w}}{\kappa_w}\frac{\gamma_w(\sigma_2)}{1\pm\gamma_w(\sigma_2)} \\ \Gamma_{i\pm}^{o,int} &= \frac{\mp 4\rho_{i\pm}^{o}}{\kappa_o}\frac{\gamma_o(\sigma_2)}{1\pm\gamma_o(\sigma_2)} \\ \Gamma_{i\pm}^{o,el} &= \frac{\mp 4\rho_{i\pm}^{o}}{\kappa_o}\frac{\gamma_o(-\sigma_1)}{1\pm\gamma_o(-\sigma_1)}\end{aligned}$$

These expressions enable us to find the grand-canonical bulk densities in water.

6.4 Grand-canonical bulk densities $\rho_{i\pm}^{w}$

In order to find the grand-canonical bulk densities in water $\rho_{i\pm}^{w}$ we impose the constraints

- $-\rho_{1-}^{w}+\rho_{1+}^{w}-\rho_{2-}^{w}+\rho_{2+}^{w}=0$ (bulk neutrality in water)
- $\rho_{1-}+\rho_{1+}=2\rho_1$
- $\rho_{2-}+\rho_{2+}=2\rho_2$
- $\rho_{1-}=\rho_{1+}$.

Note that bulk neutrality in oil is already imposed via the Donnan potential and that $\rho_{i\pm}^{o}$ are included following Eq. (6.8). The third condition, $\rho_{2-}+\rho_{2+}=2\rho_2$, follows from the system of equations (6.4). A derivation can be found in appendix B.

By imposing the four constraints given in the set of equations (6.4) we can solve for the four grand-canonical bulk densities $\rho_{i\pm}^{w}$ in water by means of a rootfinding procedure. [2]

[2] The computational package *Mathematica* (Wolfram Research Inc, Version 8), in particular, the built-in function *FindRoot* was used to solve the system of equations.

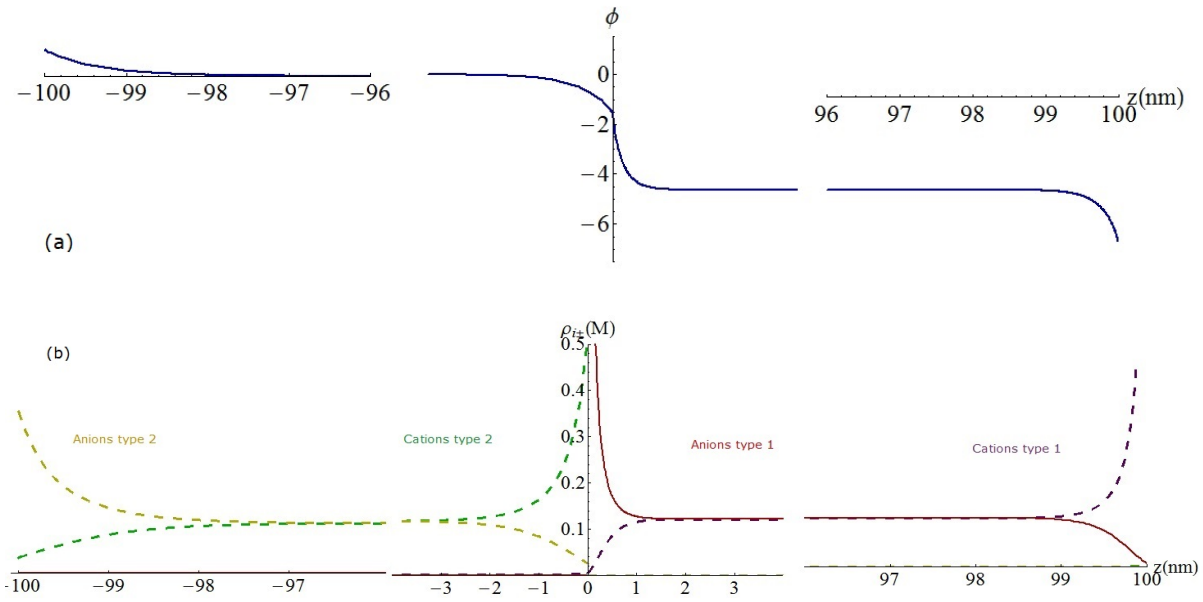

Figure 6.1: Electrostatic potential $\phi(z)$ (Fig. a) and ion distributions in units of molarity (Fig. b) in a planar slit of width $H = 200$ nm filled with water ($-\frac{H}{2} < z < 0$) and oil ($0 < z < \frac{H}{2}$). Canonical bulk densities of the salts are $\rho_1 = \rho_2 = 100$ mM, charge density on the left plate is $\sigma_1 = 0.2$ nm^{-2}. Self energies are $f_{1-} = -10$ kT, $f_{1+} = f_{2-} = 0$ and $f_{2+} = 10$ kT.

7 Experimental Studies of an electrified Interface

Summary

A connection with a recent study of an electrified oil-water interface by Laanait et al. is made in this chapter. Experiments that are relevant for this thesis are mentioned and the technicalities of applying a potential difference are explained, both experimentally and theoretically.

7.1 Experiment

Many experimental and computational studies have related theoretical models of ion concentrations near an electrified oil-water interface to the experimental investigation of these distributions. A recent paper bij Laanait et al.[3] focuses on an electrolytic cell: an electrical device that consists of two parallel electrodes and is connected to a voltage source. This cell contains an aqueous (NaCl) and an oily solution: bis(triphenylphosphoranylidene) ammonium tetrakis(pentafluorophenyl)borate (BTPPA-TPFB) in 1,2dichloroethane (DCE), separated by a planar interface. We presented such a system in section 6, albeit without the voltage source. Now we consider an additional potential difference, which is applied between bulk water and bulk oil. The experimental procedure and the subtleties of simulating an applied

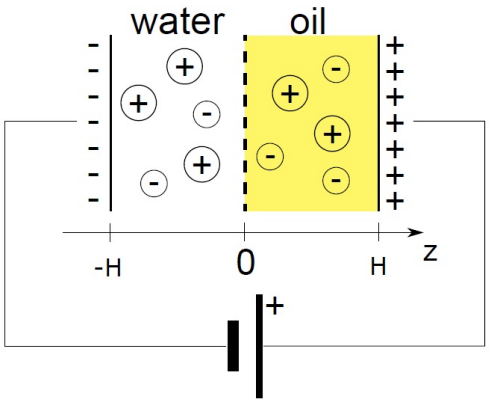

Figure 7.1: Schematic depiction of an electrolytic cell [4]

potential difference will be discussed in section 7.2. The accompanying variation in ion distributions near the oil-water interface is probed by a technique known as X Ray Reflectivity Data Analysis [8]. The so-called Wilhelmy plate method is used to measure the potential-dependent interfacial tension. From these measurements the charge accumulation near the interface is determined via the Lippmann equation [8], which will be discussed in section 11.2.

In the sections to follow we will extend our theoretical framework to fully cover this type of experiment. We will refer to this particular research project and analyse the accuracy of the PB model.

7.2 Application of the potential difference

7.2.1 The electrochemical cell: $\Delta\Phi^{wo}$

The three relevant interfaces in the electrochemical cell of present interest are those between either solution and the adjacent electrode and the oil-water interface. The experimentalists are primarily interested in the potential difference $\Delta\Phi^{wo}$ across the oil-water interface. Only the difference in electric potential between the electrons in either electrode $\Delta\Phi^{wo,cell}$ is measurable and tunable, however, since it is equal to the external voltage. The connection between the platinum electrodes ensures that $\Delta\Phi^{wo,cell}$ is zero when no external voltage is applied. A zero external voltage indicates that the sum of the voltage in- or

[3] *Tuning ion correlations at an electrified soft interface*, PNAS **109**, 20326 (2012)

decreases across the three relevant interfaces is zero: it does not indicate that $\Delta\Phi^{wo}$ is trivial. By the use of silver chloride (non-polarizable) electrodes a potential difference can, in very good approximation, be applied directly between bulk oil and bulk water. The potential of zero charge $\Delta\Phi^{pzc}$ across the oil-water interface is determined via interfacial tension measurements, as explained in section 7.1. This offset potential corresponds to zero charge accumulation σ_2 at the interface. The interfacial tension has its maximum at this point. This is apparent from the Lippmann equation, given in section 11.2. The electric potential difference $\Delta\Phi^{wo}$ is gauged so that $\Delta\Phi^{wo}\Big|_{\sigma_2=0} = 0$, hence $\Delta\Phi^{wo}$ is given by the applied potential difference across the electrochemical cell minus the potential of zero charge [6]

$$\Delta\Phi^{wo} \equiv \Delta\Phi = \Delta\Phi^{wo,cell} - \Delta\Phi^{pzc}. \tag{7.1}$$

7.2.2 Theory: ϕ_{ext} and ϕ_D

While it is experimentally feasible to apply a potential difference $\Delta\Phi^{wo,cell}$ it is theoretically convenient to impose a charge density σ_1 on the left electrode. The theoretical model that was developed in section 6 is similar but not identical to the electrochemical cell. An uncharged left electrode defines the equilibrium situation. We consider two natural notions of *potential difference*.

The externally applied potential difference between the two electrodes,

$$\phi_{ext} = \phi(\frac{H}{2}) - \phi(-\frac{H}{2})$$

can be tuned by σ_1, since this charge density determines the grand-canonical bulk densities $\rho^w_{i\pm}$.

The boundary conditions for Poisson-Boltzmann theory near the electrodes and interface, as given in Eq. (3.12) and Eq. (4.8), respectively, are such that the external potential is nonzero in equilibrium. Rather, it is the earlier encountered difference between the bulk liquids: the Donnan potential ϕ_D. This potential can be regulated by σ_1 for the same reason.

Thus, while we do not directly enforce any potential and while ϕ_D is in general not equal to ϕ_{ext}[4], both potentials can be tuned by means of a single variable. The concept of a potential of zero charge is superfluous here: a trivial Donnan potential corresponds to zero excess interfacial charge.

7.3 The canonical versus the grand-canonical ensemble

A closed system of two planar electrodes and two salts as introduced in section 6 serves as a starting point. Potential differences ϕ_{ext} (between both electrodes) and a Donnan potential ϕ_D (between bulk oil and water) are applied by means of a charge σ_1 on the left plate. The system's equilibrium state will be considered throughout this thesis.[5] The following parameters play an important role.

- Self-energies $f_{i\pm}$
- Distance H between both electrodes.
- Canonical concentrations of both salts ρ_1 and ρ_2.

We will study the effects of the aforementioned parameters on the potentials $\phi_{ext}(\sigma_1)$ and $\phi_D(\sigma_1)$ and examine the correlation coupling parameter. The consistency of our results with the study *Tuning ion correlations* can then be verified.

[4] This is only the case for high self-energies $|f_{i\pm}|$ and/or a small value of H. We will shortly come back to this point.
[5] Strictly speaking, the system is in a dynamic equilibrium. See appendix C for more information.

8 Importance of the Self-Energies for the relevant Ensemble

Summary

Charge accumulation at the water side of the oil-water interface will be used to examine the influence of the self-energies of each of the four types of ions on the suitable ensemble to describe the electrolytic cell. The grand-canonical ensemble is found to be appropriate when at least one type of ions is both hydrophilic and hydrophobic. If all four self-energies are nonzero the ensemble depends on their values: strong preferences for either phase indicate that the system is canonical.

8.1 Charge accumulation at the water side defined

Preferential partitioning of ions generates double layers near the interface, of typical widths κ_w^{-1} and κ_o^{-1} in the water and oil phases, respectively. The charge at the water side of the oil-water interface, referred to as σ_2, is given by

$$\sigma_2 = -\int_{-\frac{H}{4}}^{0} \mathrm{dz}(-\rho_{1-}^w(z) + \rho_{1+}^w(z) - \rho_{2-}^w(z) + \rho_{2+}^w(z)),$$

where we have added the overall minus sign for convenience. This parameter is useful in determining whether to treat the system in the canonical or the grand-canonical ensemble. For the system under consideration we will speak of the grand-canonical limit when the interface is effectively separated from the electrodes. In this limit σ_2 is solely determined by the Poisson-Boltzmann theory near the dielectric interface and σ_2 is constant as function of σ_1. This condition is equivalent to independence of σ_1 and the Donnan potential ϕ_D. By contrast, σ_2 and ϕ_D can be manipulated by σ_1 in the canonical ensemble. The canonical limit is attained when $\sigma_2 = \sigma_1$.

For given $N_{i\pm}$ and H the preferred ensemble depends on the self-energies. Ions may be highly hydrophilic, such as Na^+ and Cl^-, hydrophobic, such as carbon groups, or amphiphilic. These properties are reflected by the self-energies. We recall that a positive self-energy indicates a preference for water.

8.2 Two or three hydrophilic and hydrophobic ion species

We introduce the convention $f_{i\pm} = (f_{1-}, f_{1+}, f_{2-}, f_{2+})$, so all anions have a preference for water if $f_{i\pm} = (f, 0, f, 0)$, with $f > 0$, and the Donnan potential increases with f. Fig. 8.1 shows the Donnan potential as a function of σ_1 for this parameter set. Even for f as high as 40 kT the Donnan potential cannot be tuned by the external charge density.

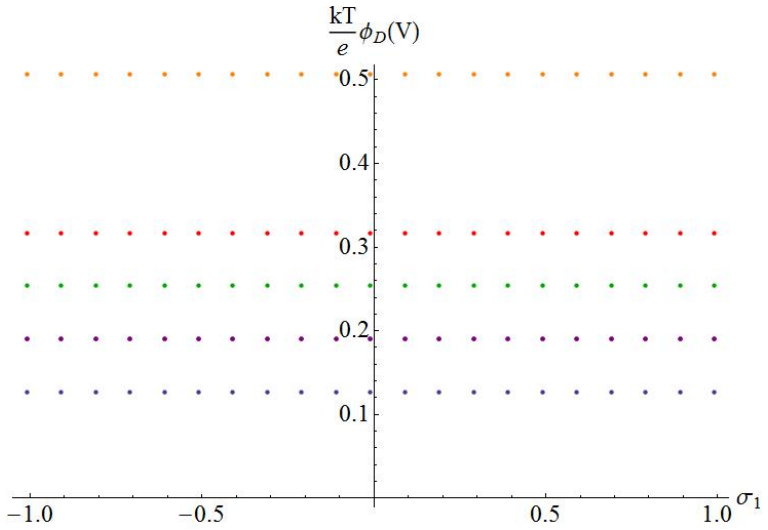

Figure 8.1: The Donnan potential as a function of the charge density σ_1 on the left electrode, for $f_{i\pm} = (f, 0, f, 0)$, $\rho_i = 10$ mM and $H = 4$ cm. From top to bottom: $f = 10, f = 15, f = 20, f = 25$ and $f = 40$ kT. The grand-canonical ensemble is appropriate for all values of f in this case, since ϕ_D is unaffected by the charge density σ_1.

Other possibilities include

1. $f_{i\pm} = (f, 0, f, 0)$ (all anions hydrophilic)
2. $f_{i\pm} = (0, -f, 0, 0)$ (cations type 1 hydrophobic)
3. $f_{i\pm} = (-f, 0, 0, f)$ (anions type 1 hydrophilic, cations type 2 hydrophobic)

For parameter set 1 the external potential is positive in equilibrium due to the anions' preference for water. If only one of the self-energies is unequal to zero the absolute values of ϕ_{ext} are relatively small. The Donnan potential as a function of σ_1 is shown in Fig. 8.2 for $f = 23$ kT. The sign of ϕ_D can be read off from the self-energies. For $f_{i\pm} = (-23, 0, 0, 23)$ kT, for instance, the type one anions have a preference for water, while the type two cations are more likely to be found in oil. These self-energies indice a negative Donnan potential. A constant $\phi_D(\sigma_1)$ indicates that the system is grand-canonical.

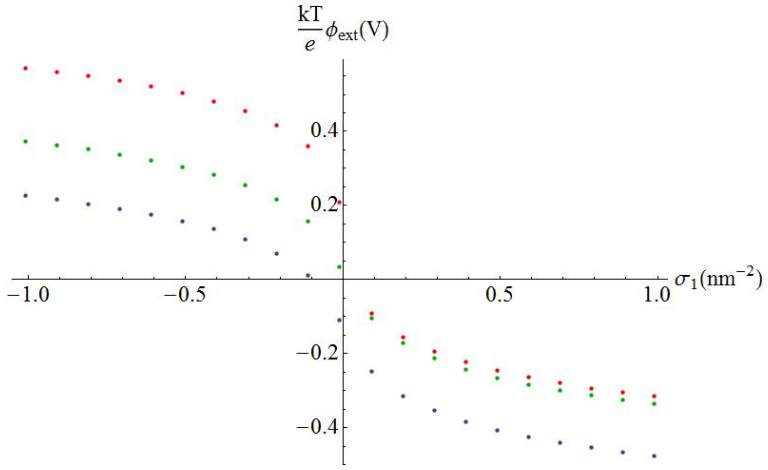

Figure 8.2: The external potential as a function of the charge density σ_1 on the left electrode, for $\rho_i = 10$ mM and $H = 4$ cm. From top to bottom: $f_{i\pm} = (10, 0, 10, 0)$ kT, $f_{i\pm} = (0, -10, 0, 0)$ kT and $f_{i\pm} = (0, -10, 0, 0)$ kT.

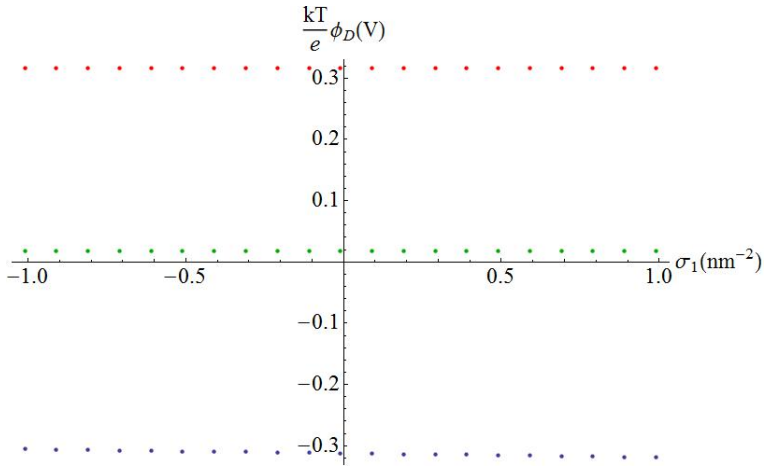

Figure 8.3: The Donnan potential as a function of the charge density σ_1 on the left electrode, for $\rho_i = 10$ mM and $H = 4$ cm. From top to bottom: $f_{i\pm} = (23, 0, 23, 0)$ kT, $f_{i\pm} = (0, -23, 0, 0)$ kT and $f_{i\pm} = (-23, 0, 0, 23)$ kT. Even for f as high as 23 kT the system is grand-canonical when two or more self-energies are equal to zero.

8.3 The contrast between $(-f, 0, 0, f)$ and $(-f, -f, f, f)$

There is an essential difference between a system where two out of four ion species have an affinity with both phases and one where a distinction between a hydrophobic and an hydrophilic salt can be made. For a macroscopic system with $H = 4$ cm and fixed $\rho_i = 10$ mM the grand-canonical ensemble would be the obvious choice for $f_{i\pm} = (-f, 0, 0, f)$. For the latter parameter set the ensemble depends entirely on the value of f. This point is illustrated in Fig. 8.4. If one ion species is amphiphilic (without a preference for either phase) the effect on σ_2 (σ_1) is very similar to the presence of two amphiphilic species: it makes σ_2 independent of σ_1.

The suitability of either ensemble depends largely on the length H. As a general rule, the validity of the grand-canonical approximation at fixed $f_{i\pm}$ increases with the system size. Special attention to the role of the system size will be paid in section 9.

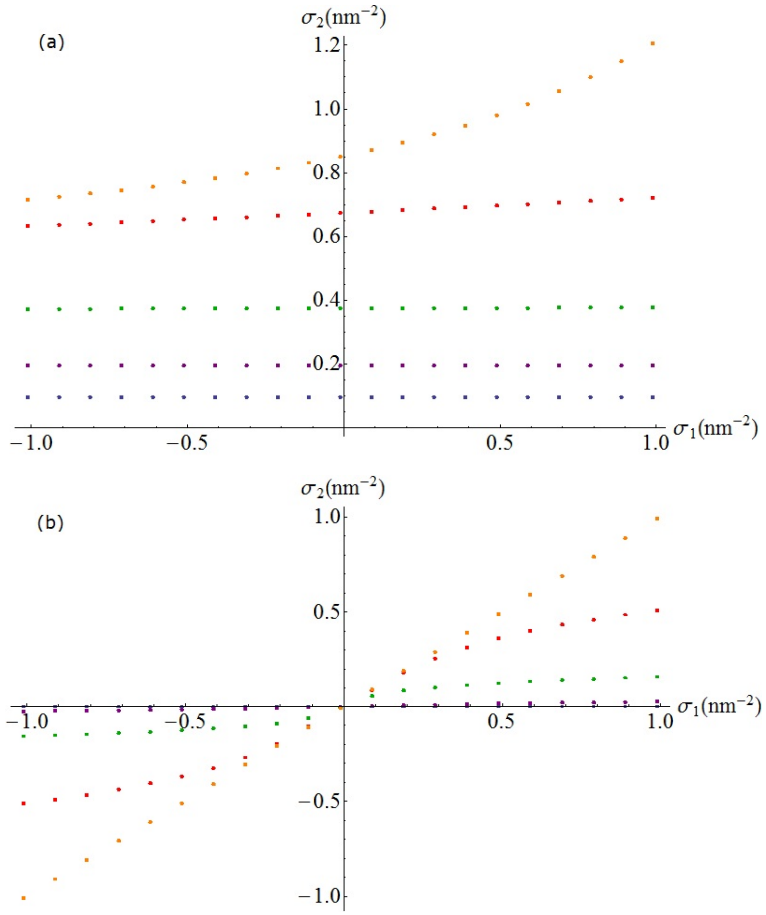

Figure 8.4: Charge density σ_2 near the interface as a function of the density σ_1 on the left electrode for $H = 4$ cm and $\rho_i = 10$ mM. a) Self-energies are given by $f_{i\pm} = (-f, 0, 0, f)$. From top to bottom: $f = 40$, $f = 25$, $f = 20$, $f = 15$ and $f = 10$ kT. Canonical effects only begin to show for self-energies well above 25 kT. b)Self-energies are given by $f_{i\pm} = (-f, -f, f, f)$; $f = 40$, $f = 25$, $f = 20$, $f = 15$ and $f = 10$ kT. The curve for $f = 10$ kT is constant and equal to zero by symmetry of the self-energies; σ_1 has a noticeable effect on σ_2 for $f \geq 20$ kT. The system is perfectly canonical for $f = 40$ kT.

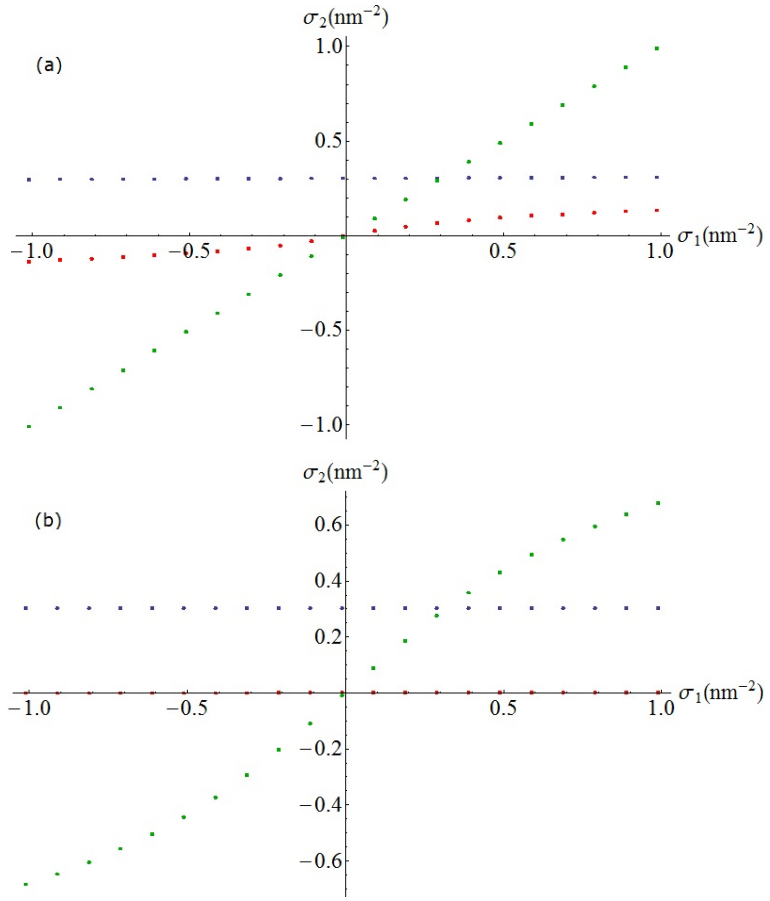

Figure 8.5: Density $\sigma_2(\sigma_1)$ for $\rho_i = 10$ mM. a)$H = 10^4$ nm. The linear (canonical) curve represents $f_{i\pm} = (-23, -23, 23, 23)$ kT, whereas the system is entirely grand-canonical for $f_{i\pm} = (-10, 0, 0, 10)$ kT (flat curve). Slight canonical effects are apparent for $f_{i\pm} = (-10, -10, 10, 10)$ kT. Note that the charge density σ_2 is nonzero in the grand-canonical limit for the case of two amphiphilic ions; no net charge builds up in this limit if the two salts have equal but opposite preferences. b)$H = 1$ cm. The curves for $f_{i\pm} = (-10, 0, 0, 10)$ kT and $f_{i\pm} = (-10, -10, 10, 10)$ kT are perfectly grand-canonical for this system size. Canonical effects begin to show for $f_{i\pm} = (-23, -23, 23, 23)$ kT.

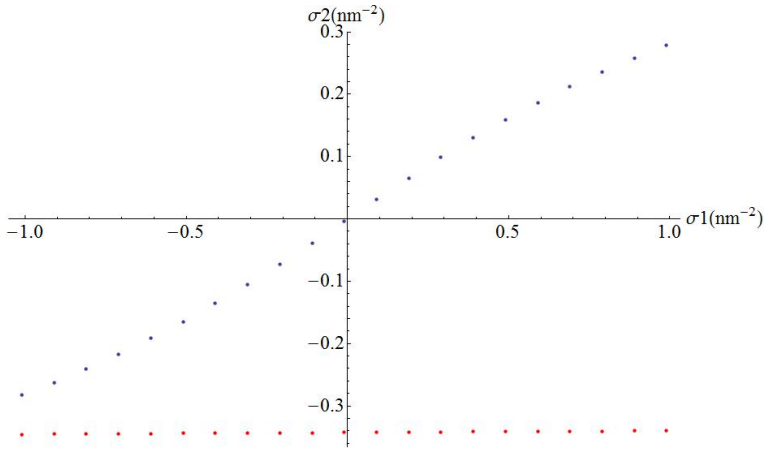

Figure 8.6: Charge density σ_2 as a function of σ_1 for $H = 4$ cm and $\rho_i = 100$ mM. For $f_{i\pm} = (-20, -20, 20, 20)$ kT the relation is linear, while $f_{i\pm} = (-20, -20, 20, 0)$ kT gives rise to a grand-canonical system.

9 Importance of the System Size for the relevant Ensemble

Summary

We study the effects of the system size, characterized by the difference between the two planar electrodes, on the choice of ensemble. The system turns out to become more grand-canonical for larger values of this length. A crossover length marking the transition between the canonical and the grand-canonical ensemble is defined and the dependence of this crossover length on the self-energies is investigated. The potential difference between the electrodes and the Donnan potential as functions of the system size are shown to increase notably at the crossover length.

9.1 Tunableness of interfacial excess charge

Keeping self-energies $f_{i\pm}$ and canonical bulk densities $\rho_i = \frac{N_i}{AH}$ fixed we study the dependence of σ_2 on σ_1 for different values of H. The presence of a positive charge density σ_1 induces the adsorption of anions on the left electrode, leading to a decrease in ρ_{i-}^w and making σ_2 less negative. For small values of H the density σ_2 is linearly related to σ_1 by charge neutrality. Note that $\lim_{H\to 0}$ is not a physical limit for this model since this does not allow for a bulk electrolyte. The number of particles $N_{i\pm}$ increases linearly with H as we take ρ_i to be constant. A large value of H thus implies the availability of many ions to screen σ_1 and the effect of σ_2 on σ_1 should become insignificant.

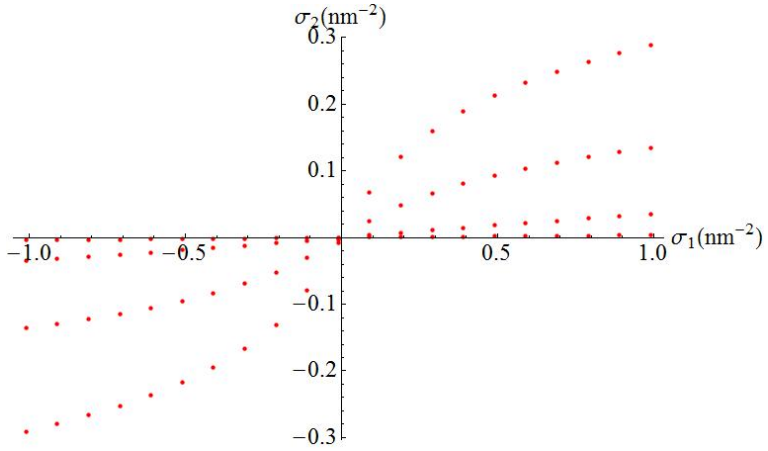

Figure 9.1: Charge accumulation σ_2 as a function of σ_1 for self-energies $f_{i\pm} = (-10, -10, 10, 10)$ kT; $\rho_i = 10$ mM. The flat curve corresponds to $H = 10^6$ nm; increasingly steeper graphs show $H = 10^5$, $H = 10^4$ and $H = 10^3$ nm, respectively.

9.2 Crossover H

In brief, we distinguish between the canonical and grand-canonical limits as follows

Grand-canonical limit	**Canonical limit**
Density σ_2 constant	Density $\sigma_2 = \sigma_1$
Macroscopic length scale (typically $H \simeq 1 - 10$ cm)	Microscopic length scale (typically $H \simeq 100 - 1000$ nm)
Self-energies $\lvert f_{i\pm}\rvert \simeq 0$	Self-energies $\lvert f_{i\pm}\rvert \gg 1$

Large values of the system's length H account for minimal influence of σ_1 on σ_2, since essentially infinite amounts of ions will be available for screening. As H becomes larger the system moves towards the grand-canonical end of the spectrum. For fixed values of $f_{i\pm}$ we define a crossover length H^*, such that we speak of the grand-canonical regime for $H > H^*$.

Determination of the crossover length H^* is best illustrated graphically. At $H = H^*$ a transition between the canonical and grand-canonical regime takes place.[6]

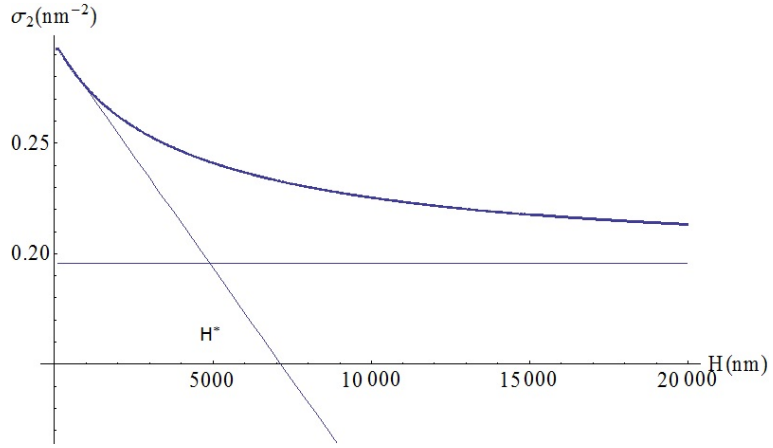

Figure 9.2: Linear graph showing σ_2 (nm^{-2}) as a function of the length H (nm) and the value σ_2 attains in the limit of infinite H (constant function) for $\rho_i = 10$ mM, $\sigma_1 = 0.3$ nm^{-2} and $f_{i\pm} = (-15, 0, 0, 15)$ kT. The crossover length H^* is given by the value of H where the line tangent to the curve at small H and the limiting (grand-canonical) value of σ_2 intersect.

By means of this procedure crossover lengths for $f_{i\pm}$ of the form $(-f, 0, 0, f)$ were calculated. The results are shown in Fig. 9.3.

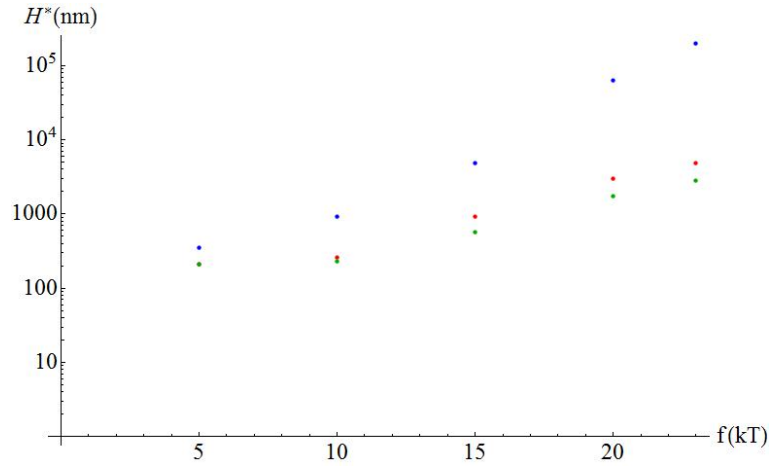

Figure 9.3: Logarithmic graph of crossover lenghts as a function of f, where $f_{i\pm} = (-f, 0, 0, f)$, for $\sigma_1 = 0.3$ nm^{-2} and for $\rho_i = 10$ mM (top curve), $\rho_i = 100$ mM (middle curve) and $\rho_i = 1$ M (bottom curve). The length H^* appears exponential in f.

The relation $H^* \simeq \log f$ becomes more obvious when we consider $f_{i\pm} = (-f, -f, f, f)$. The crossover length grows faster for this parameter set, as anticipated.

Taking $f_{i\pm} = (-f, -f, 20, 20)$ kT we let f run from 20 to 30 kT in Fig. 9.5 to study the effects of such an asymmetry on H^*. The crossover length initially increases with f, and it reaches a constant value at $f \simeq 26$ kT. For $f \gg 20$ kT species 2 can pass through the interface at a relatively low energetic cost and will respond to changes in σ_1.

[6]This model is reliable for H as small as 10 nm; values smaller than 100 nm have not been included in this fit. For $H \leq 100$ nm the density σ_2 grows with H, for the simple reason that more ions become available for accumulation at the interface. Curves that include these data do not allow for proper tangent lines.

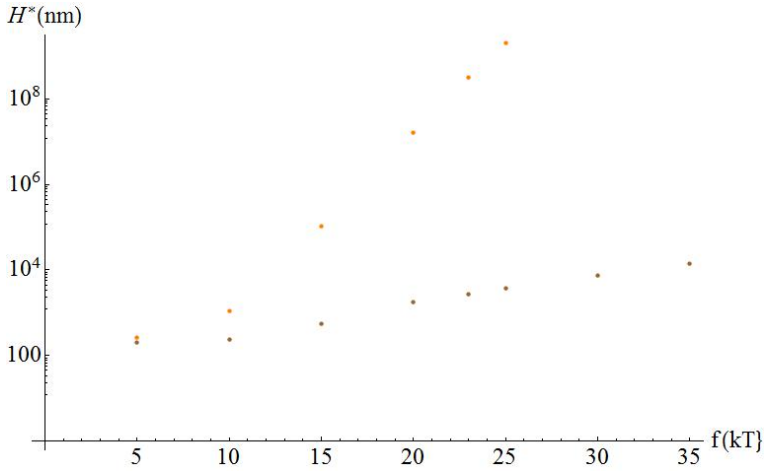

Figure 9.4: Logarithmic graph of crossover lengths as a function of f, where $f_{i\pm} = (-f, -f, f, f)$ (top curve) and $f_{i\pm} = (-f, 0, 0, f)$ (bottom curve), for $\sigma_1 = 0.3$ nm^{-2} and $\rho_i = 1$ M.

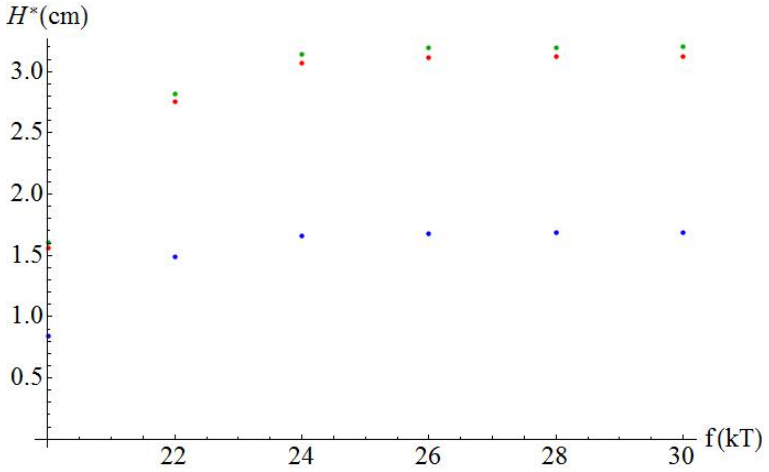

Figure 9.5: Crossover length H^* (cm) as a function of f, where self-energies are given by $f_{i\pm} = (-f, -f, 20, 20)$ kT, for $\sigma_1 = 0.3$ nm^{-2} and $\rho_i = 100$, $\rho_i = 500$ and $\rho_i = 1000$ mM. For $f \geq 26$ kT the crossover length is controlled by $f_{2\pm}$.

9.3 Potential differences ϕ_D and ϕ_{ext}

The crossover length is apparent in the effect of H on the Donnan potential ϕ_D and the external potential ϕ_{ext}. At fixed $f_{i\pm}$ and σ_1 the Donnan potential, given by equation (6.2), increases with the system size. There is a critical range for H where enough ions become available for the screening of σ_1. The system increases its Donnan potential and the external potential follows. This process terminates at the crossover length. For these parameters $H^* = 0.85 * 10^6$ nm.

Figure (9.7) shows the impact of H on $\phi_D(\sigma_1)$. Greater values of H reduce the influence of the density σ_1 on the Donnan potential, as expected. The Donnan potential at the crossover length is shown by the middle curve.

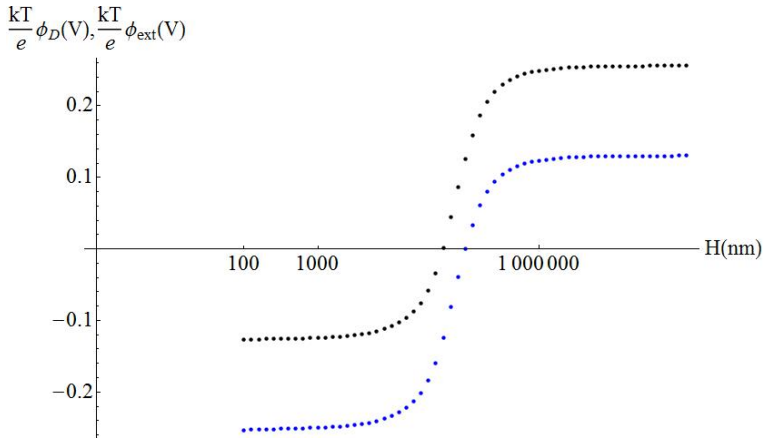

Figure 9.6: Potentials $\frac{kT}{e}\phi_D$ (V) (top curve) and $\frac{kT}{e}\phi_{ext}$ (V) (bottom curve) as a function of the system's length H (nm) for $f_{i\pm} = (-20, -20, 20, 20)$ kT, $\sigma_1 = 0.3$ nm^{-2} and $\rho_i = 100$ mM. The Donnan potential increases with H and reaches a constant value at $H^* = 0.85 * 10^6$ nm.

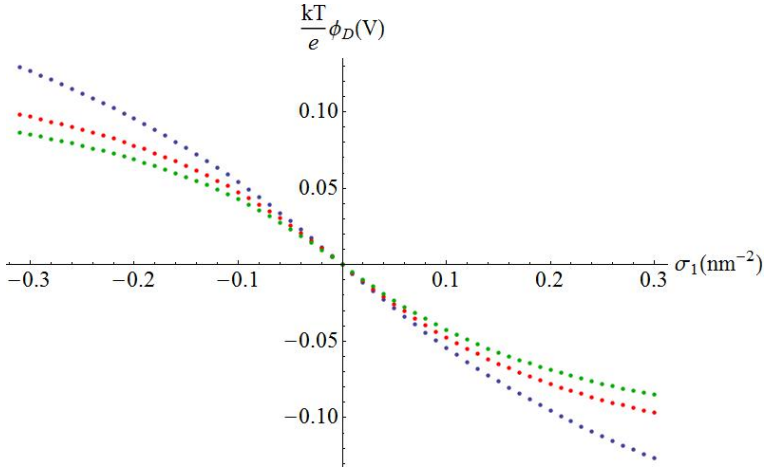

Figure 9.7: Donnan potential ϕ_D as a function of charge density σ_1 for $\rho_i = 100$ mM, $f_{i\pm} = (-20, -20, 20, 20)$ kT for $H = 100$ nm (linear curve), $H = H^* = 0.85$ cm (crossover curve) and $H = 1.8$ cm (gradual curve).

10 Tunable ion-solvent Interactions near the Interface

Summary

The experiments of Nouamane Laanait, Mark Schlossman and others [7] formed a direct motivation to study the electrolytic cell in more detail. In this section comparisons are made between theoretical and experimental results. The electrolytic cell is shown to be nearer the canonical than the grand-canonical end of the spectrum. Within our PB description the system becomes grand-canonical if two out of four self-energies are set to zero. Predictions of the interfacial excess charge as a function of the Donnan potential by Poisson-Boltzmann theory become less accurate as the latter increases. Calculations of the correlation coupling parameters suggest that improvement of the PB model could be made by including ion-ion correlations between the hydrophobic ions near the interfaces, where ion densities are high.

10.1 Experimental parameters

In the previously mentioned publication *Tuning ion at an electrified soft interface* an electrolytic cell of length $H = 4$ cm containing aqueous ($\epsilon_w = 78.54$) and organic ($\epsilon_o = 10.43$) electrolyte solutions is considered at $T = 294$ K. Sodium chloride was dissolved in water to produce a 10 mM solution. A solution of BTPPATPFB in DCE was prepared at a concentration of 5 mM. Because of the low dielectric constant of DCE only partial dissociation into $BTPPA^+$ and $TPFB^-$ occurs, producing an organic solution with a dissociated ionic concentration of 2.7 mM [7].

The authors include three energy terms for the ions: electrostatic, ion-solvent potential of mean force $f_{i\pm}^{sol}$ and excess chemical potential due to ion correlations μ^{corr}. Including f_{1+}^{sol} or f_{2-}^{sol} had little or no effect on the data analyses in this setting, so these parameters were usually excluded.[7] The equation for the density profiles $\rho_{i\pm}$ takes the form [7]

$$\rho_{i\pm}(z) = \rho_{i\pm}^{bulk} \exp[\mp\phi(z) - f_{i\pm}^{sol} - \mu^{corr}].$$

This relation reduces to our PB relation of Eq. (4.6 if we ignore the ion correlations by setting $\mu^{corr} = 0$. The ion-solvent potentials of mean force $f_{i\pm}^{sol}$ describe the interactions of each ionic species with the solvent; these are functions of the distance z from the interface. The potentials of mean force (PMFs) were modeled by a molecular dynamics (MD) simulation [7]. An example is given in Fig. 10.1.

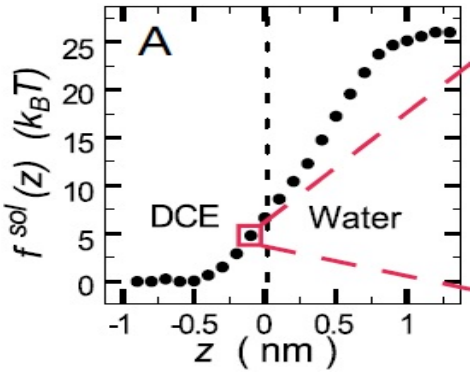

Figure 10.1: Ion-solvent potential of mean force (PMF) of a $TPFB^-$ ion at the water-DCE interface. Points were calculated by an MD simulation [7].

10.2 Interfacial excess charge, density profiles and potentials

In this thesis the self-energies $f_{i\pm}$ are defined as step functions. In order to simulate this experiment the differences between the bulk values of the PMFs should be used. These numbers are known as the Gibbs

[7] Thanks to Mark Schlossman for pointing this out to me.

free energies of transfer. For NaCl and BTPPATPFB these self-energies are given by [8]

$$(f_{\mathrm{TPFB}^-}, f_{\mathrm{BTPPA}^+} f_{\mathrm{Cl}^-} f_{\mathrm{Na}^+}) = (-29.9, -22.9, 22.3, 21.2)\ \mathrm{kT}$$

We will study three parameter sets of the self-energies

1. $f_{i\pm} = (-29.9, 0, 0, 21.2)$ kT (Gibbs free energies of transfer, where self-energies of BTPPA^+ and Cl^- have been set to zero)
2. $f_{i\pm} = (-29.9, -22.9, 22.3, 21.2)$ kT (experimental values of the Gibbs free energies)
3. $f_{i\pm} = (-49.9, -42.9, 42.3, 41.2)$ kT (Gibbs free energies after addition of 20 kT: the canonical limit is appropriate for these self-energies)

The first striking feature of a Fig. 10.2, which contrasts these self-energies, is the difference between set (1) on the one hand and (2) and (3) on the other hand. In parameter set (1) two ions can pass through the interface at no energetic cost. When a potential difference is applied the TPFB^- and Na^+ ions can stay in their preferred phases, while the system's electrostatic energy is minimized by the redistributions of the species BTPPA^+ and Cl^-. By contrast, σ_1 has a noticeable influence on σ_2 when $\left|f_{i\pm}\right| > 20$ kT. Thus f_{2-} and f_{1+} cannot be set to zero for a mean-field PB description. The canonical limit is also shown in Fig. 10.2, for $\left|f_{i\pm}\right| \simeq 40$ kT. The difference between both ensembles is immediate from the

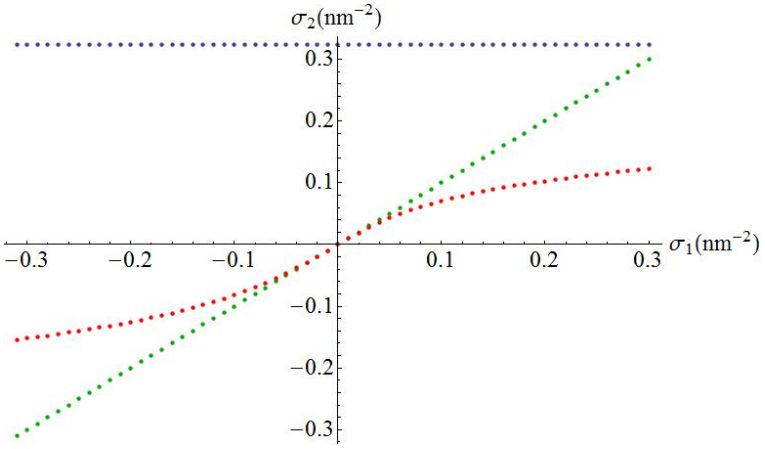

Figure 10.2: Charge density σ_2 near the interface as a function of density σ_1 on the left electrode for $H = 4$ cm, contrasing $f_{i\pm} = (-29.9, 0, 0, 21.2)$ kT (constant: grand-canonical), $f_{i\pm} = (-29.9, -22.9, 22.3, 21.2)$ kT (almost entirely canonical) and $f_{i\pm} = (-49.9, -42.9, 42.3, 41.2)$ kT (linear: canonical). Canonical densities are $\rho_1 = 2.7$ mM (oily solution) and $\rho_2 = 5$ mM (aqueous solution). Compare to Fig. 8.2.

density profiles. For parameter set (1), whose density profiles are given by the dashed line in figure (10.3) there is no accumulation of the species with zero self-energies near the interface. The density profiles for parameter sets (1) and (2) are almost identical near the electrodes. Figure 10.4 shows the relation between the imposed charge density σ_1 and the resulting potential difference between the electrodes $\phi\left(\frac{H}{2}\right) - \phi\left(\frac{H}{2}\right)$. Grand-canonical PB calculations were also done. The grand-canonical bulk densities were approximated by the canonical concentrations and the potential difference between the electrodes was defined as

$$\phi_{ext}(\sigma_1) = -\left[2\log\left(\frac{1+C_o(\sigma_1)}{1-C_o(\sigma_1)}\right) + 2\log\left(\frac{1+C_w(\sigma_1)}{1-C_w(\sigma_1)}\right)\right],$$

where the integration constants C_w and C_o are given by equation (4.11). As the self-energies increase it becomes easier to tune ϕ_{ext} by adjusting σ_1. The transition between the grand-canonical and canonical ensemble is also visible in the Donnan potential ϕ_D as a function of ϕ_{ext} in Fig. 10.5. The potential difference between the bulk phases is the potential we should really work with in order to mimic the experiment.

[8] Thanks to Mark Schlossman for providing these numbers.

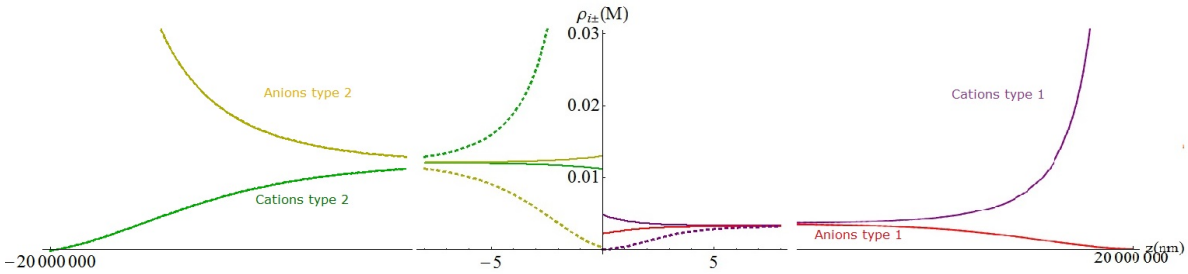

Figure 10.3: Density profiles of all ion species for $\sigma_1 = 0.3$ nm^{-2} for self-energies $f_{i\pm} = (-29.9, -22.9, 22.3, 21.2)$ kT (dashed lines) and$f_{i\pm} = (-29.9, 0, 0, 21.2)$ kT (thick lines) at $\frac{kT}{e}\phi_{ext} = -0.54$ V and $\frac{kT}{e}\phi_{ext} = -0.44$ V, respectively.

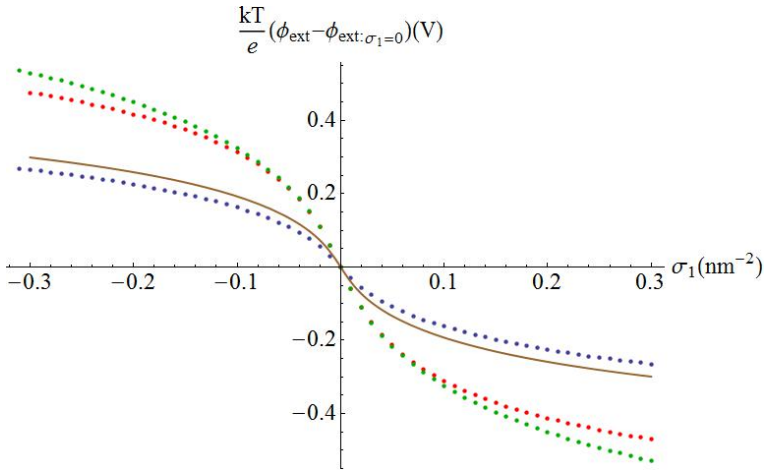

Figure 10.4: The potential difference between the electrodes $\frac{kT}{e}\phi_{ext}$ for $H = 4$ cm as a function of σ_1, for grand-canonical (smooth curve) and canonical (dotted curves) PB theory, the latter for $f_{i\pm} = (-29.9, 0, 0, 21.2)$ kT (bottom curve), $f_{i\pm} = (-29.9, -22.9, 22.3, 21.2)$ kT and $f_{i\pm} = (-49.9, -42.9, 42.3, 41.2)$ kT (steepest curve). The charge density has a maximal effect on the potential for larger $f_{i\pm}$. All data points have been translated by the corresponding Donnan potential at $\sigma_1 = 0$.

In the canonical limit ϕ_D is equal to ϕ_{ext}. The Donnan potential is equivalent to the experimental $\Delta\Phi$ (as defined in Eq. (7.1)) for self-energies $f_{i\pm} = (-49.9, -42.9, 42.3, 41.2)$ kT, since both potentials are applied directly between the bulk phases. In Fig. 10.6 the charge accumulation at the water side of the interface σ_2 is shown for a suitable range of potential differences: experimentally $\left|\Delta\Phi\right| \leq 0.406$ V. The data were obtained by application of a potential difference $\Delta\Phi$ between the bulk phases, a potential that is not well-defined in our theoretical PB model. It makes a difference whether we compare the data with σ_2 ($\frac{kT}{e}\phi_{ext}$) or with σ_2 ($\frac{kT}{e}\phi_D$), as Fig. 10.6 shows. Although not directly applied the Donnan potential is a potential between the bulk phases. From Fig. 10.6 we see that mean field Poisson-Boltzmann theory predicts too high a charge density, especially for high values of the Donnan potential. A possibility to improve this model is discussed in section 10.3.

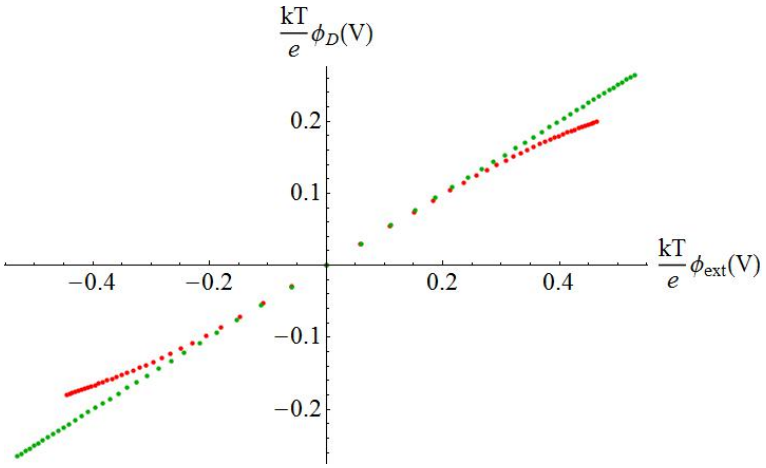

Figure 10.5: Donnan potential $\frac{kT}{e}\phi_D$ as a function of the applied potential ϕ_{ext} between the plates, for $f_{i\pm} = (-29.9, -22.9, 22.3, 21.2)$ kT and $f_{i\pm} = (-49.9, -42.9, 42.3, 41.2)$ kT (linear curve). A potential difference can be applied directly between bulk water and bulk oil for the present parameter choice ($f_{i\pm}$ large enough and small enough system size $H < H^*$).

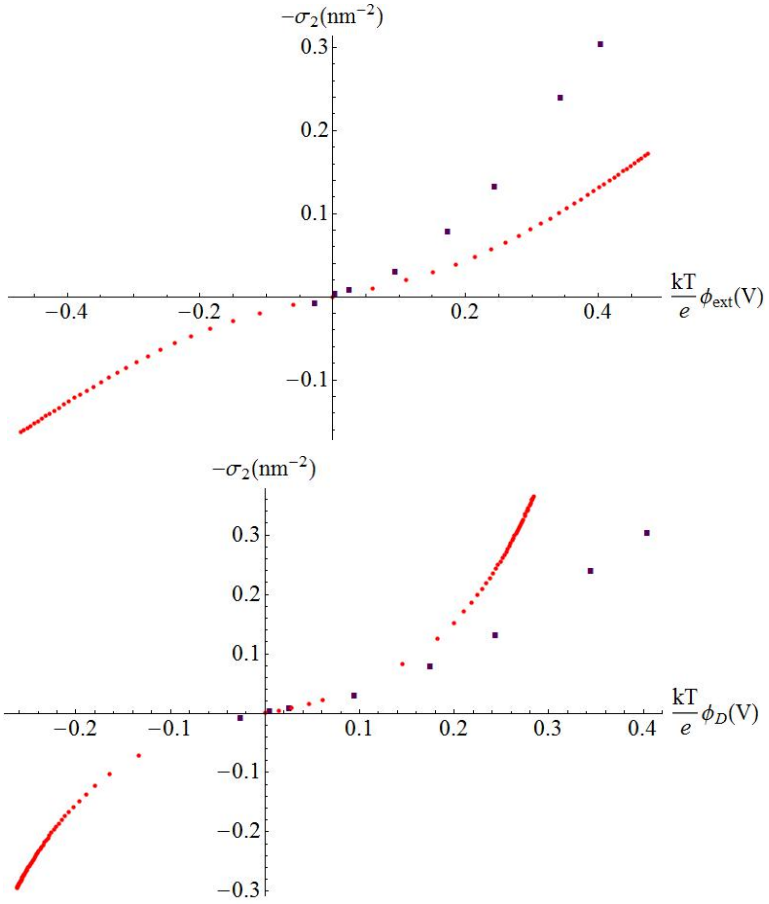

Figure 10.6: Charge accumulation σ_2 as a function of the potential differences $\frac{kT}{e}\phi_{ext}$ (a) and $\frac{kT}{e}\phi_D$ (b), for self-energies $f_{i\pm} = (-29.9, -22.9, 22.3, 21.2)$ kT and $f_{i\pm} = (-49.9, -42.9, 42.3, 41.2)$ kT (steep curve). Experimental data (square symbols) are shown as a function of $\Delta\Phi$ between bulk oil and bulk water.

10.3 Correlation Coupling Parameter

Correlations between ions are characterized by the correlation coupling parameter Γ. The oil and water phases can be modelled as one component plasmas (OCPs) for this purpose. An OCP consists of N ions carrying charge e in a uniform neutralizing background of volume V and dielectric constant ϵ. The average ionic density is $\rho = \frac{N}{V}$. The advantage of working with the OCP is that it only contains two independent length scales: the average separation between the particles $d = (\frac{4\pi\rho}{3})^{-\frac{1}{3}}$ and the Bjerrum length λ_B [9]. The dimensionless correlation coupling parameter (CCP) is given by

$$\Gamma = \frac{\lambda_B}{d}.$$

Ion correlations caused by their electrostatic interactions are expected to be important when the average electrostatic interaction energy between neighbouring ions is larger than the thermal energy kT [7]; this situation corresponds to $\Gamma > 1$. Poisson-Boltzmann theory holds in the limit $\Gamma \ll 1$. Although Ion-ion correlations are usually considered to be irrelevant for monovalent ions in aqueous solution, the lower relative permittivity of the organic DCE ($\epsilon_r = 10.43$) generates a large coupling strength Γ [7]. Correlations are negligible for ions far from the interface, because bulk concentrations are low [7].

Calculations for the CCPs of the ion species of interest as a function of z were done for the parameters of Fig. 10.7. For $\phi_{ext} > 0$ correlations between $TPFB^-$ ions are relevant, indicating that our mean-field PB model could be improved by accounting for these ion-ion correlations. The CCPs can be tuned by

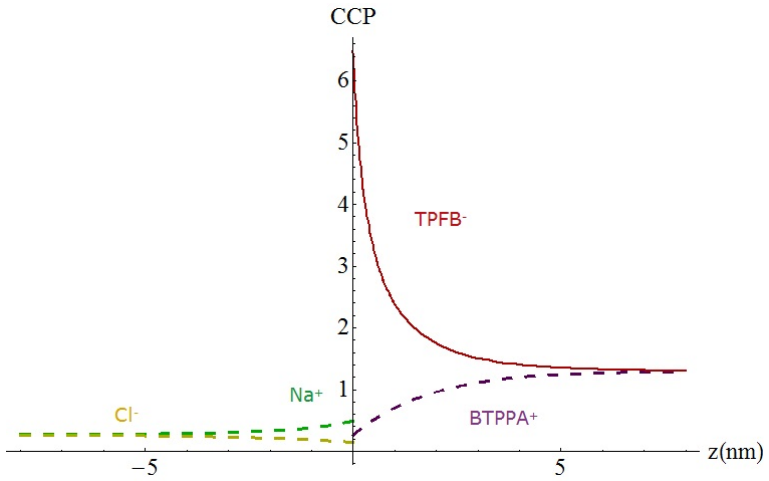

Figure 10.7: Correlation coupling parameters as a function of z nm near the oil-water interface, for $\phi_{ext} = 0.4$ V, for $f_{i\pm} = (-29.9, -22.9, 22.3, 21.2)$ kT, $\rho_1 = 2.7$ mM, $\rho_2 = 10$ mM and $H = 4$ cm. A change in sign of ϕ_{ext} interchanges the roles of cat- and anions in either phase.

the application of an external potential. In Fig. 10.8 the correlation coupling parameter for $TPFB^-$ near the interface is shown for different values of the external potential ϕ_{ext}. When no potential is applied $\Gamma \simeq 1$ and the system is accurately described by Poisson-Boltzmann theory.

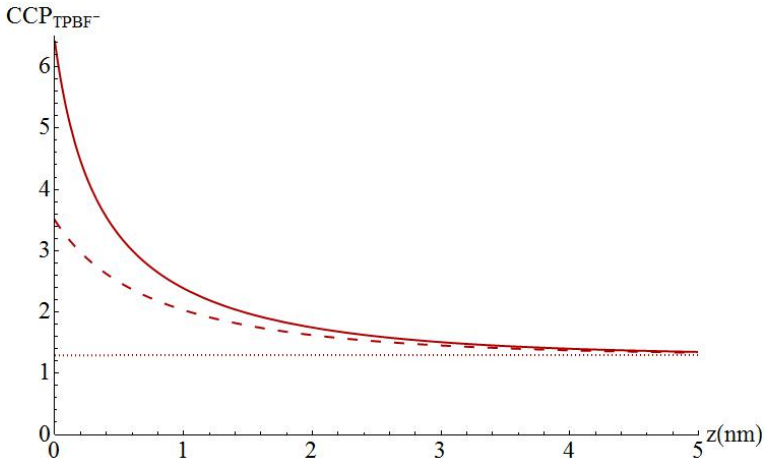

Figure 10.8: The correlation coupling parameter for ions of type $TPFB^-$ as a function of z (nm) for $\phi_{ext} = 0$ (dotted line), $\phi_{ext} = 0.2$ V (dashed line) and $\phi_{ext} = 0.4$ V (thick line), for $f_{i\pm} = (-29.9, -22.9, 22.3, 21.2)$ kT, $\rho_1 = 2.7$ mM, $\rho_2 = 10$ mM and $H = 4$ cm.

11 Surface Tension within the Electrolytic Cell

Summary

There are (at least) two ways to calculate the surface tension of the oil-water interface in the electrochemical cell. It can either be derived from the grand-potential functional (3.4) or obtained from the Lippmann equation. Agreement between these two methods is shown to be good. Both appear to be in agreement with the experimental data.

11.1 Transformed potential βY

For a calculation of the surface tension of each of the relevant interfaces within the electrochemical cell we rearrange the terms in Eq. (3.4) as

$$\beta\Omega[\{\rho_\alpha\}] = \int_V \mathrm{d}\mathbf{r}\rho_+(\mathbf{r})\left(\frac{\rho_+(\mathbf{r})}{\rho_s} - 1 + \beta V_+\Big(\mathbf{r})\right) + \int_V \mathrm{d}\mathbf{r}\rho_+(\mathbf{r})\left(\frac{\rho_+(\mathbf{r})}{\rho_s} - 1 + \beta V_-(\mathbf{r})\right) + \frac{1}{2}\int_V \mathrm{d}\mathbf{r}Q(\mathbf{r})\phi(\mathbf{r}).$$

For a description of the electrochemical cell the potential $\beta Y[\{\mu_\alpha\}, \phi_{ext}]$ is obtained from a Legendre transformation

$$\beta Y[\{\mu_\alpha\}, \phi_{ext}] = \beta\Omega[\{\rho_\alpha\}] - \int_V \mathrm{d}\mathbf{r}\phi(\mathbf{r})q(\mathbf{r}), \tag{11.1}$$

where $q(\mathbf{r}) = q(z) = \sigma\delta\left(z + \frac{H}{2}\right) - \sigma\delta\left(z - \frac{H}{2}\right)$, describes the electrode charges, such that

$$-\int_V \mathrm{d}\mathbf{r}\phi(\mathbf{r})q(\mathbf{r}) = \frac{A}{2}\sigma\phi_{ext}.$$

From the equilibrium condition $\frac{\delta Y}{\delta\rho_\pm} = 0$ we regain the Boltzmann distributions (3.9). Note that the charge density q is independent of $\rho_\pm(z)$ within the description of the system by the grand potential Y, while ϕ_{ext} varies with these distributions. The equilibrium potential is found by inserting the equilibrium density profiles and taking into consideration that $\rho_\pm^o = \rho_o \exp[\mp(\phi(z) - \phi_D)]$

$$\begin{aligned}\frac{\beta Y_{eq}}{A} &= \int_{-\frac{H}{2}}^{0} \mathrm{d}z\rho_w\phi(z)\sinh\phi(z) - \int_{-\frac{H}{2}}^{0} \mathrm{d}z\left\{2\rho_w[\cosh\phi(z) - 1]\right\} - \frac{\sigma}{2}\phi\left(-\frac{H}{2}\right) \\ &+ \int_0^{\frac{H}{2}} \mathrm{d}z\rho_o\phi(z)\sinh(\phi(z) - \phi_D) - \int_0^{\frac{H}{2}} \mathrm{d}z\left\{2\rho_o\left[\cosh(\phi(z) - \phi_D) - 1\right]\right\} + \frac{\sigma}{2}\phi\left(\frac{H}{2}\right).\end{aligned}$$

Using the relation $\beta\gamma = \beta Y_{eq} - \beta Y\big|_{\rho=\rho_{w,o}}$ we acquire the dimensionless surface tension $\beta\gamma$

$$\begin{aligned}\frac{\beta\gamma}{A} &= \int_{-\frac{H}{2}}^{0} \mathrm{d}z\rho_w\phi(z)\sinh\phi(z) - \int_{-\frac{H}{2}}^{0} \mathrm{d}z\left[2\rho_w\cosh\phi(z)\right] - \frac{\sigma}{2}\phi\left(-\frac{H}{2}\right) \\ &+ \int_0^{\frac{H}{2}} \mathrm{d}z\rho_o\phi(z)\sinh(\phi(z) - \phi_D) - \int_0^{\frac{H}{2}} \mathrm{d}z\left[2\rho_o\cosh(\phi(z) - \phi_D)\right] + \frac{\sigma}{2}\phi\left(\frac{H}{2}\right).\end{aligned} \tag{11.2}$$

The surface tension comprises four contributions which can be straightforwardly separated for the case at hand:

$$\begin{aligned}\beta\gamma^{el,w} &= \int_{-\frac{H}{4}}^{-\frac{H}{4}} \mathrm{d}z\rho_w\phi(z)\sinh\phi(z) - \int_{-\frac{H}{2}}^{-\frac{H}{4}} \mathrm{d}z\left[2\rho_w\cosh\phi(z)\right] - \frac{\sigma}{2}\phi\left(-\frac{H}{2}\right) \\ \beta\gamma^{w,int} &= \int_{-\frac{H}{4}}^{0} \mathrm{d}z\rho_w\phi(z)\sinh\phi(z) - \int_{-\frac{H}{4}}^{0} \mathrm{d}z\left[2\rho_w\cosh\phi(z)\right] \\ \beta\gamma^{int,o} &= \int_0^{\frac{H}{4}} \mathrm{d}z\rho_o\phi(z)\sinh(\phi(z) - \phi_D) - \int_0^{\frac{H}{4}} \mathrm{d}z\left[2\rho_o\cosh(\phi(z) - \phi_D)\right] \\ \beta\gamma^{o,el} &= \int_{\frac{H}{4}}^{\frac{H}{2}} \mathrm{d}z\rho_o\phi(z)\sinh(\phi(z) - \phi_D) - \int_{\frac{H}{4}}^{\frac{H}{2}} \mathrm{d}z\left[2\rho_o\cosh(\phi(z) - \phi_D)\right] + \frac{\sigma}{2}\phi\left(\frac{H}{2}\right).\end{aligned} \tag{11.3}$$

The interfacial tension, given by the sum of $\beta\gamma^{w,int}$ and $\beta\gamma^{int,o}$, depends on σ_1 via the potential ϕ and the bulk densities ρ_w and ρ_o. The curve in Fig. 11.1,, as follows from Eq. (11.3), should be vertically translated by an experimental constant: the interfacial tension is nonzero when no external potential is applied.

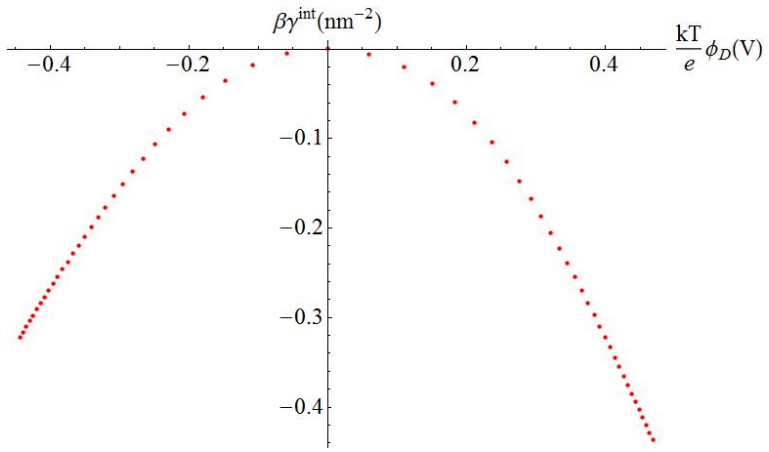

Figure 11.1: Interfacial tension $\beta\gamma^{int} = \beta\gamma^{w,int} + \beta\gamma^{int,o}$ as a function of the external potential in volts for $f_{i\pm} = (-29.9, -22.9, 22.3, 21.2)$ kT, $\rho_1 = 2.7$ mM, $\rho_2 = 10$ mM and $H = 4$ cm, based on relations (11.3).

11.2 Lippmann equation

The Lippmann equation

$$\sigma_2 = -\left(\frac{\partial\gamma^{int}}{\partial\phi_D}\right)_{T,V,\mu_i} \tag{11.4}$$

relates the tension at the oil-water interface to the interfacial excess charge σ_2 at fixed chemical potentials μ_i [8]. The interfacial tension can thus be obtained from

$$\gamma^{int} = -\int \mathrm{d}\phi_\mathrm{D}\sigma_2. \tag{11.5}$$

There is good agreement between the interfacial tension as defined by the grand-canonical Lippmann equation (11.5) and γ^{int} as given by the oil-water terms of (11.3). For the conversion to dynes/cm, which was made for Fig. 11.2 density $e\sigma_2$ was used, as opposed to the number density σ_2. This change affects the units of the tension:

$$[\gamma] = [e\sigma_2][\frac{kT}{e}\phi_D] = \frac{\mathrm{CV}}{\mathrm{nm}^2},$$

where

$$1\frac{\mathrm{CV}}{\mathrm{nm}^2} = 10^{18}\frac{\mathrm{J}}{\mathrm{m}^2} = 10^{18}\frac{\mathrm{N}}{\mathrm{m}} = 10^{21}\frac{\mathrm{dynes}}{\mathrm{cm}}.$$

A constant of 28.3 dynes/cm was added to the interfacial tension.[9] Surface tension measurements and the interfacial tension as derived from the Lippmann equation are compared in Fig.(11.3). Qualitatively similar results are found for small values of the applied potential $\Delta\Phi$.

[9]This translation was made based on the measurements in *Tuning ion correlations at an electrified soft interface: supplementary information.*

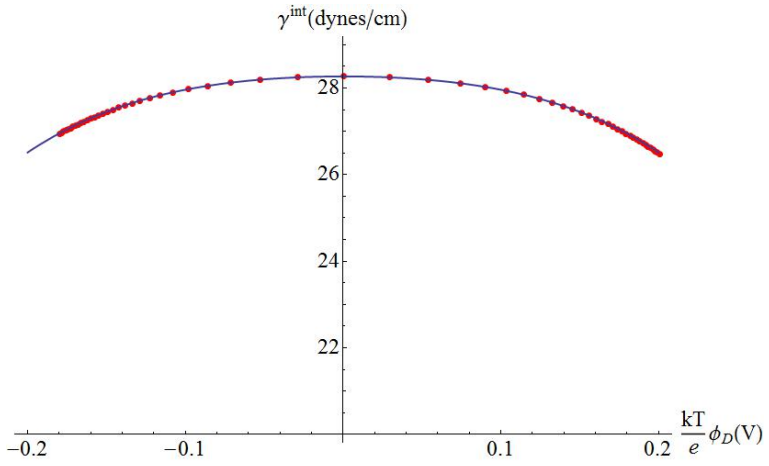

Figure 11.2: Interfacial tension $\beta\gamma^{int}(\phi_D)$ as given by relations (11.3) (line) and by Eq. (11.5) (dots) for $f_{i\pm} = (-29.9, -22.9, 22.3, 21.2)$ kT, $\rho_1 = 2.7$ mM, $\rho_2 = 10$ mM and $H = 4$ cm.

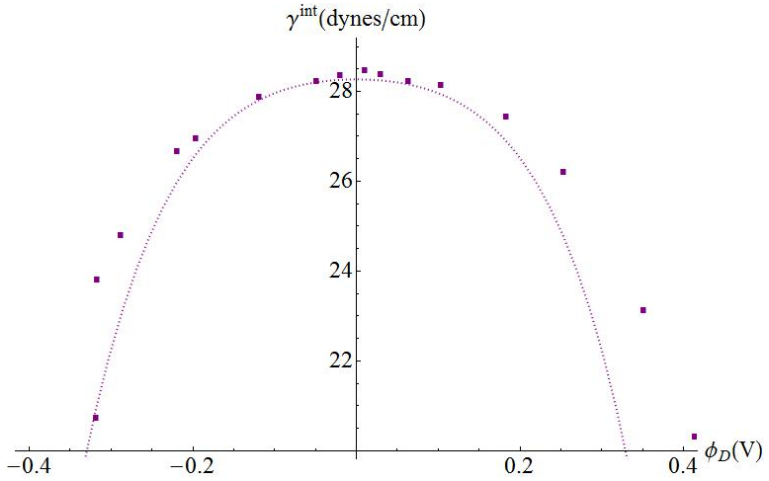

Figure 11.3: The interfacial tension γ^{int} as a function of the Donnan potential as derived from the Lippmann equation (11.5) (dotted line) and as measured at the oil-water interface of an electrolytic cell [8], for $f_{i\pm} = (-29.9, -22.9, 22.3, 21.2)$ kT, $\rho_1 = 2.7$ mM, $\rho_2 = 10$ mM and $H = 4$ cm. Data were translated by the potential of zero charge $\Delta\Phi^{pzc}$. An experimental constant of 28.3 dynes/cm was added to the results of the Lippmann equation in order to account for the bare oil-water tension.

12 Conclusions and Outlook

Throughout this thesis we studied monovalent ions near electrodes and oil-water interfaces by means of nonlinear Poisson-Boltzmann theory, which describes the electrostatic potential and density profiles near these surfaces. Self-energies were introduced to describe ion-solvent interactions. Antagonistic salts with different signs of self-energies of cations and anions, were associated with small Debye lengths and a strongly decreasing effect on the oil-water interfacial tension.

Poisson-Boltzmann theory was applied to study a finite system with the possibility of applying a potential difference across the oil-water interface. This description would enable us to simulate experiments recently done by Laanait et al. [7] The appropriate ensemble to treat this system in was shown to depend on both the self-energies and the system length. We examined the conditions for a canonical treatment of the electrochemical cell. One of these were one strongly hydrophilic and one strongly hydrophobic salt, reflected in high values of the ions' self-energies. Another important condition was a system length well below the crossover length, which was defined to mark the transition from the canonical to the grand-canonical ensemble.

These insights were applied to the experiments done by Laanait et al., leading to the conclusion that the canonical ensemble should be used for a Poisson-Boltzmann description of this system. Comparisons with experimental data of the charge accumulation at the water side of the interface showed that there was room for improvement in the PB model. Calculations of the correlation coupling parameters indicated that ion-ion correlations in the oil phase should be included.

Finally, expressions for the oil-water interfacial tension were derived from the theory developed in early chapters. Good agreement between the result of this derivation and available data was found. The Lippmann equation, which was taken from literature, also appeared suitable for this purpose. A derivation of this expression would be the cherry on the cake.

References

[1] M. Bier et al., *Liquid-liquid interfacial tension of electrolyte solutions*, Phys.Rev.Lett. **101**, 046104 (2008).

[2] N. Boon, *Electrostatics in ionic solution*, PhD thesis (2012). Utrecht University.

[3] L.C. Filion, *Advanced Statistical Physics*, lecture notes (2012). Utrecht University.

[4] I.C. Gârlea, *Dynamics of charged particles in an electrolytic cell with an oil-water interface*, master thesis (2010). Utrecht University.

[5] J.N. Israelachvili, *Intermolecular and surface forces*, 2nd edition (page 37). London: Academic Press (1991).

[6] N. Laanait et al., *Communications: Monovalent ion condensation at the electrified liquid/liquid interface*, J.Chem.Phys., **132**, 171101 (2010).

[7] N. Laanait et al., *Tuning ion correlations at an electrified soft interface*, PNAS, **109**, 20326-20331 (2012).

[8] N. Laanait et al. (2012), *Tuning ion correlations at an electrified soft interface*, supplementary information. Retrieved from *http://www.pnas.org/content/early/2012/11/21.*

[9] Y. Levin (2002), *Electrostatic correlations: from plasma to biology*, Rep.Prog.Phys. **65**, 1577-1632 (2002).

[10] G. Luo et al., *Ion Distributions near a Liquid-Liquid Interface*, Science **311**, 216-218 (2006).

[11] R. van Roij, *Advanced Statistical Physics*, lecture notes and problems. Utrecht University (2012).

[12] R. van Roij, *Soft Condensed Matter Theory*, lecture notes and problems. Utrecht University (2010).

[13] R. van Roij, *Statistical thermodynamics of supercapacitors and blue engines*, Cornell University Library (2012). Retrieved from *http://arxiv.org/abs/1211.1269.*

[14] R.D. Weir et al., *Electrochemistry at the interface between two immiscible electrolyte solutions* (IUPAC Technical Report), Pure Appl. Chem., **76**, 2147-2180 (2004).

[15] J.W. Zwanikken, *Looking deeper into emulsions and suspensions*, PhD thesis. Utrecht University (2009).

Acknowledgements

My decision to start my first research project at the Institute for Theoretical Physics was met by more than one discouraging face. When I was told that theoretical physics was not the field a bachelor student should go into I became all the more curious. I thought my critics were right when I opened my first source - a PhD thesis - and they would probably have turned out right if it hadn't been for my fantastic supervisors. Modest statues of René van Roij and Niels Boon in the Minnaert building's main hall would be appropriate.

I would like to thank René for making me enthusiastic for this project and for sharing my enthusiasm throughout the year. I was particularly impressed when he handed me some of his calculations on the surface tension and asked me to return them before the weekend. Thanks, René, for the many hours you spent on guiding me in the right direction and teaching me the statistical physics I needed. Thank you for taking my input seriously and for repeatedly implying that my understanding of the Poisson-Boltzmann description of the electrolytic cell was as good as yours.

It would be hard to exaggerate Niels's role, who found some of the most persistent bugs in my notebooks. On the Friday before Christmas, when I was close to deleting my code for the charge density near the interface, Niels stayed at the ITP until 7.30 p.m. and fixed it. He too was genuinely happy with the result. Niels, thank you for your intuitive explanations of ions' behaviour near electrodes and interfaces. Thank you for your detailed checks of my calculations and for making me feel slightly insecure by putting my ideas up for discussion.

When I was struggling with the paper *Tuning ion correlations at an electrified soft interface* a lot of help came from one of the authors, from the University of Chicago. Mark Schlossman's incredibly fast, elaborate and friendly replies to my emails have made a significant contribution towards my comprehension of current experimental research on ion distributions near an oil-water interface. I am indebted to Ben Erné and Mark Vis for showing me the electrolytic cell from a chemist's point of view. I am grateful to Jeffrey for introducing me to soft matter and to PB theory in particular and to Rick for his demonstrations of the construction of tangent lines in *Mathematica*. Finally, I would like to thank my parents for their unceasing encouragement and support.

A Derivations in Poisson-Boltzmann Theory

A.1 The Boltzmann distributions

These distributions can be obtained from the equilibrium condition $\frac{\delta\beta\Omega[\{\rho_\alpha\}]}{\delta\rho_+} = 0$. The variation of Eq. (3.1) with respect to $\rho_+(\mathbf{r})$ is found by substituting $\rho_+(\mathbf{r}) \to \rho_+(\mathbf{r}) + \delta\rho_+(\mathbf{r})$:

$$\begin{aligned}
\beta\Omega[\{\rho_\alpha\}] \;\to\; & \int \mathrm{d}\mathbf{r}(\rho_+(\mathbf{r}) + \delta\rho_+(\mathbf{r}))\left[\log\left(\rho_+(\mathbf{r}) + \delta\rho_+(\mathbf{r})\Lambda_+^3\right) - 1\right] \\
+ \;& \lambda_B \int \mathrm{d}\mathbf{r} \int \mathrm{d}\mathbf{r}' \frac{(\rho_+(\mathbf{r}) + \delta\rho_+(\mathbf{r}) - \rho_-(\mathbf{r}) + \sigma\delta(z))(\rho_+(\mathbf{r}') + \delta\rho_+(\mathbf{r}') - \rho_-(\mathbf{r}') + \sigma\delta(z))}{|\mathbf{r} - \mathbf{r}'|} \\
+ \;& \beta \int \mathrm{d}\mathbf{r}\left[((\rho_+(\mathbf{r}) + \delta\rho_+(\mathbf{r}))(V_+(\mathbf{r}) - \mu_+) + \rho_-(\mathbf{r})(V_-(\mathbf{r}) - \mu_-)\right],
\end{aligned}$$

where we have used that $\mathbf{r}$ and $\mathbf{r}'$ are dummy variables. Inserting the first order expansion $\log(\rho_+ + \delta\rho_+) \simeq \log(\rho_+) + \frac{1}{\rho_+}\delta\rho_+$ and collecting terms we find

$$\begin{aligned}
\beta\Omega[\{\rho_\alpha\}] \;\to\; & \int \mathrm{d}\mathbf{r}\rho_+(\mathbf{r})\left[\log\left(\rho_+(\mathbf{r})\Lambda_+^3\right) - 1\right] + \int \mathrm{d}\mathbf{r}\delta\rho_+(\mathbf{r})\log\left(\rho_+(\mathbf{r})\Lambda_+^3\right) \\
+ \;& \lambda_B \int\int \mathrm{d}\mathbf{r}\mathrm{d}\mathbf{r}'\left(\frac{Q_+(\mathbf{r})Q_+(\mathbf{r}')}{|\mathbf{r} - \mathbf{r}'|} + \frac{\delta\rho_+(\mathbf{r})Q_+(\mathbf{r}')}{|\mathbf{r} - \mathbf{r}'|}\right) \\
+ \;& \beta \int \mathrm{d}\mathbf{r}\left[(\rho_+(\mathbf{r})(V_+(\mathbf{r}) - \mu_+) + \rho_-(\mathbf{r})(V_-(\mathbf{r}) - \mu_-))\right] + \int \mathrm{d}\mathbf{r}\delta\rho_+(\mathbf{r})(V_+(\mathbf{r}) - \mu_+),
\end{aligned}$$

hence

$$\begin{aligned}
\delta\beta\Omega[\{\rho_\alpha\}] \;=\; & \int \mathrm{d}\mathbf{r}\delta\rho_+(\mathbf{r})\log\left(\rho_+(\mathbf{r})\Lambda_+^3\right) + \lambda_B \int \mathrm{d}\mathbf{r}\left(\int \mathrm{d}\mathbf{r}'\frac{Q_+(\mathbf{r}')}{|\mathbf{r} - \mathbf{r}'|}\right)\delta\rho_+(\mathbf{r}) \\
+ \;& \beta \int \mathrm{d}\mathbf{r}(V(\mathbf{r}) - \mu_+)\delta\rho_+(\mathbf{r}),
\end{aligned} \tag{A.1}$$

where $\lambda_B \int \mathrm{d}\mathbf{r}' \frac{Q_+(\mathbf{r}')}{|\mathbf{r}-\mathbf{r}'|} = \phi(\mathbf{r})$. The equilibrium condition thus translates into

$$\log\left(\rho_+(\mathbf{r}\Lambda_+^3)\right) + \phi(\mathbf{r}) + \beta(V_+(\mathbf{r}) - \mu_+) = 0.$$

Since $\beta\mu_+ = \log\left(\rho_s\Lambda_\pm^3\right)$ this implies

$$\rho_+(\mathbf{r}) = \rho_s \exp(-\phi(\mathbf{r}) - \beta V_\pm(\mathbf{r})).$$

B Additional constraint for the bulk densities

By definition of the adsorptions $\Gamma_{i\pm}$ we have

$$-\Gamma_{1-} + \Gamma_{1+} - \Gamma_{2-} + \Gamma_{2+} = 0, \tag{B.1}$$

which is similar to relation 3.20. Using equation $B.1$ relation 6.4 can be rewritten in the form

$$\begin{aligned}
\frac{H}{2}\left(\rho^w_{1-} + \rho^o_{1-}\right) + \frac{1}{H}\Gamma_{1-} &= \frac{H}{2}\left(\rho^w_{1-} - \rho^w_{1+} + \rho^o_{1-} - \rho^o_{1+}\right) \\
\frac{H}{2}\left(\rho^w_{1-} - \rho^w_{1+} + \rho^o_{1-} - \rho^o_{1+}\right) &= \frac{1}{H}\left(\Gamma_{1+} - \Gamma_{1-}\right) \\
\frac{H}{2}\left(\rho^w_{1-} - \rho^w_{1+} + \rho^o_{1-} - \rho^o_{1+}\right) + \frac{1}{H}\left(\Gamma_{2+} - \Gamma_{2-}\right) &= 0.
\end{aligned} \tag{B.2}$$

Finally, using charge neutrality in bulk water and bulk oil,

$$\begin{aligned}
\frac{H}{2}\left(\rho^w_{1+} + \rho^o_{1+}\right) + \frac{1}{H}\Gamma_{2-} &= \frac{H}{2}\left(\rho^w_{1-} + \rho^o_{1-}\right) + \frac{1}{H}\Gamma_{2+} \\
\frac{H}{2}\left(\rho^w_{2-} + \rho^o_{2-}\right) + \frac{1}{H}\Gamma_{2-} &= \frac{H}{2}\left(\rho^w_{2+} + \rho^o_{2+}\right) + \frac{1}{H}\Gamma_{2+} \\
\rho_{2-} &= \rho_{2+}.
\end{aligned} \tag{B.3}$$

C The steady state

The main properties of the electrochemical cell are shown schematically in figure $C.1$. The electrodes consist of platinum wires attached to square platinum meshes [6]. A potential difference is applied between

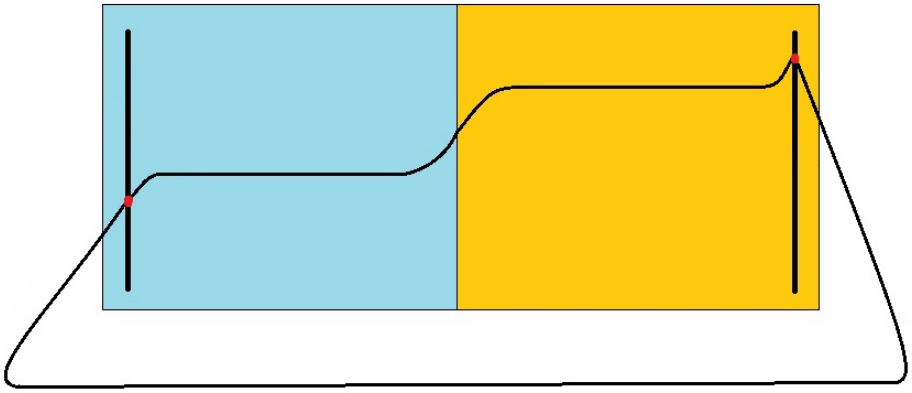

Figure C.1: Electrochemical cell diagram: a potential difference is applied between the electrodes. A typical potential ϕ is shown.

the electrodes; this results in a charge density σ_1 on the left plate. In this example $\sigma_1 < 0$. A suitable ion species will respond to the new situation. In the experiment under consideration there will be a flow of Cl^- ions from water to oil. Briefly, there is a strong current and $\rho^w_{Cl^-}$ decreases as a result. The depletion of Cl^- ions must be compensated for in order for the system to meet the imposed voltage. This is done by means of redox reactions. Anions with a strong affinity for water, such as OH^-, and cations with a preference for oil are created in water and oil, respectively. This induces a net negative current from water to oil, which in turn gives rise to more redox reactions: a dynamic equilibrium. The equilibrium current is typically very weak ($\simeq 1 - 10\ \mu$A) and will not be taken into account.

D Derivation of the Lippmann equation

The electrolytic cell can be described by the potential $Y[\{\mu_i\}, \phi_{ext}]$, as defined in section (11.1). The corresponding differential is given by

$$dY = -\mathrm{N_i d}\mu^{\mathrm{i}} - \mathrm{pdV} + \gamma \mathrm{dA} - \sigma \mathrm{Ad}\phi_{\mathrm{ext}}, \tag{D.1}$$

where γ denotes the total surface tension. The relation

$$\mathrm{Y}[\{\mu_{\mathrm{i}}\}, \phi_{\mathrm{ext}}] = -\mathrm{p}[\{\mu_{\mathrm{i}}\}]\mathrm{V} + \gamma[\{\mu_{\mathrm{i}}\}, \phi_{\mathrm{ext}}]\mathrm{A} \tag{D.2}$$

holds by the extensivity of V and A. Combining equations (D.1) and (D.2) leads to

$$-\mathrm{N_i d}\mu^{\mathrm{i}} - \sigma \mathrm{Ad}\phi_{\mathrm{ext}} = -\mathrm{Vdp} + \mathrm{Ad}\gamma. \tag{D.3}$$

We note that $\mathrm{N_i} = (\rho_{\mathrm{i}}^{\mathrm{w}} + \rho_{\mathrm{i}}^{\mathrm{o}})\mathrm{AH} + \Gamma_{\mathrm{i}}\mathrm{A}$, hence the terms that scale with A in Eq. (D.3) can be separated from those linear in V:

$$\begin{cases} (\rho_{\mathrm{i}}^{\mathrm{w}} + \rho_{\mathrm{i}}^{\mathrm{o}})\mathrm{d}\mu^{\mathrm{i}}\mathrm{AH} = \mathrm{Vdp} \\ -\Gamma_{\mathrm{i}}\mathrm{d}\mu_{\mathrm{i}} - \sigma \mathrm{d}\phi_{\mathrm{ext}} = \mathrm{d}\gamma. \end{cases} \tag{D.4}$$

Collecting interfacial terms from the second relation in (D.4) gives

$$\mathrm{d}\gamma^{\mathrm{int}} = -\sigma_2 \mathrm{d}\phi_{\mathrm{D}} - \Gamma_{\mathrm{i}}\mathrm{d}\mu^{\mathrm{i}},$$

which yields the grand-canonical Lippmann equation $\mathrm{d}\gamma^{\mathrm{int}} = -\sigma_2 \mathrm{d}\phi_{\mathrm{D}}$ at constant chemical potentials. The canonical Lippmann equation in integral form becomes

$$\gamma^{int} = -\int \mathrm{d}\phi_{\mathrm{D}}\sigma_2 - \int \mathrm{d}\mu^{\mathrm{i}}\Gamma_i^{int}. \tag{D.5}$$

The interfacial tension is directly obtained from this relation when $\sigma_2(\phi_D)$ and $\Gamma_i(\mu_i)$ are known.